Assessing the time of emergence of global ocean fish biomass using ensemble climate to fish simulations

Nicolas Barrier[1], Olivier Maury[2], Roland Séférian[3], Yeray Santana-Falcón[4], and Matthieu Lengaigne[5]

[1]MARBEC, Univ. Montpellier, CNRS, Ifremer, IRD
[2]Institut de Recherche pour le Développement
[3]CNRM (Météo-France/CNRS)
[4]Centre National de Recherches Météorologiques
[5]MARBEC

April 01, 2024

Abstract

Climate change is anticipated to considerably reduce global marine fish biomass, driving marine ecosystems into unprecedented states with no historical analogues. The Time of Emergence (ToE) marks the pivotal moment when climate conditions (i.e. signal) deviate from pre-industrial norms (i.e. noise). Leveraging ensemble climate-to-fish simulations, this study examines the ToE of epipelagic, migratory and mesopelagic fish biomass, alongside their main environmental drivers, for two contrasted climate-change scenarios. Globally-averaged biomass signals emerge over the historical period. Epipelagic biomass decline emerges earlier (1950) than mesozooplankton decline (2000) due to a stronger signal in the early 20th century, possibly related to trophic amplification induced by an early-emerging surface warming (1915). Trophic amplification is delayed for mesopelagic biomass due to postponed warming in the mesopelagic zone, resulting in a later emergence (2000). ToE displays strong size class dependence, with medium sizes (20 cm) experiencing delays compared to the largest (1 m) and smallest (1 cm) categories. Regional signal emergence lags behind the global average, with median ToE estimates of 2029, 2034 and 2033 for epipelagic, mesopelagic and migrant communities, respectively, due to systematically larger local noise compared to global one. These ToEs are also spatially heterogeneous, driven predominantly by the signal pattern, akin to mesozooplankton. Additionally, our findings underscore that mitigation efforts (i.e. transitioning from SSP5-8.5 to SSP1-2.6 scenario) have a potential to curtail emerging ocean surface signals by 40%.

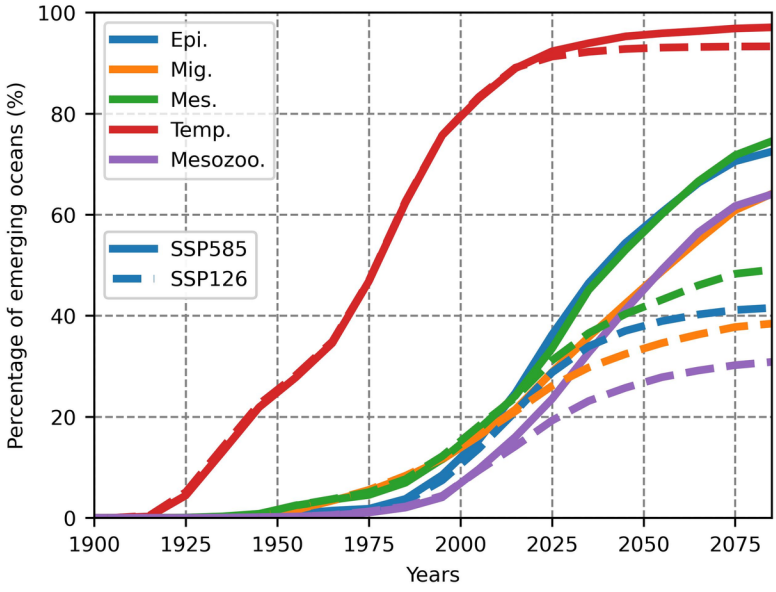

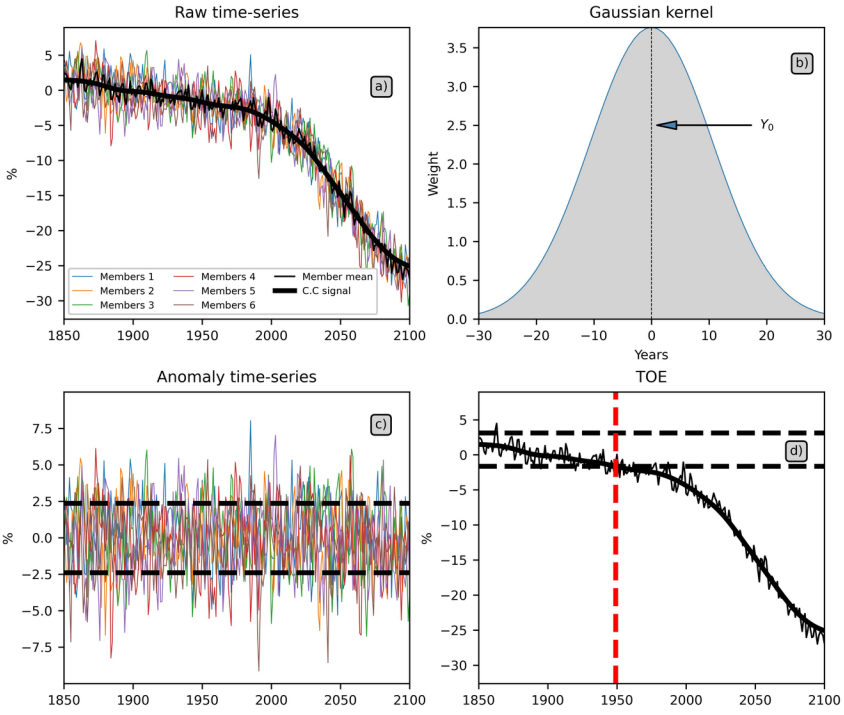

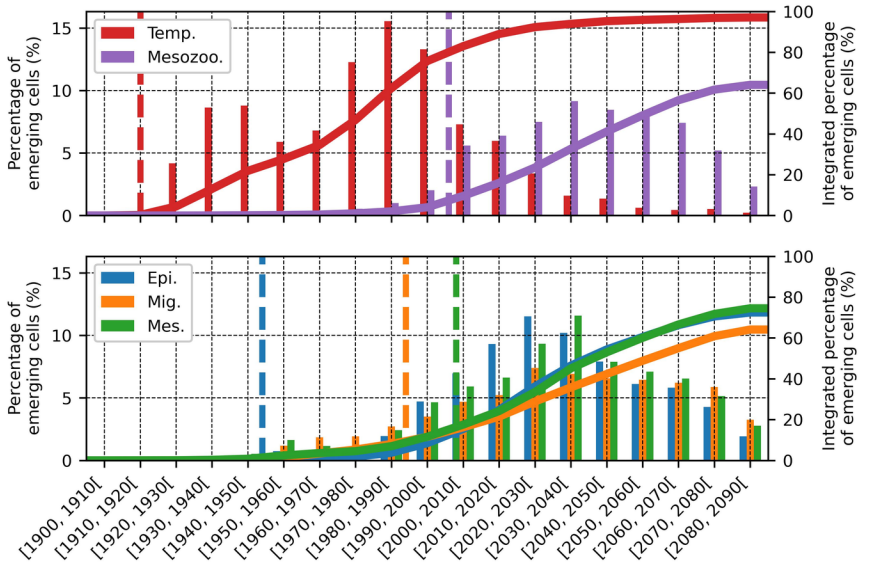

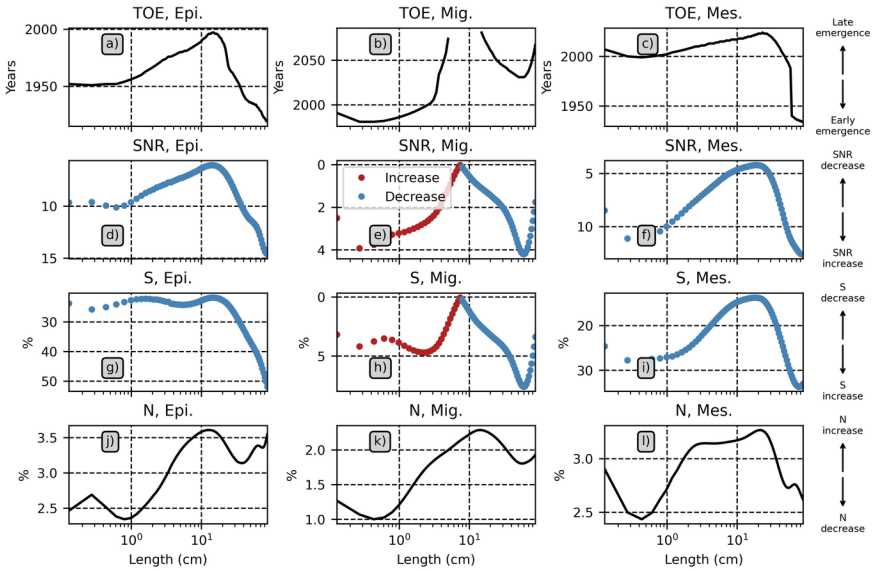

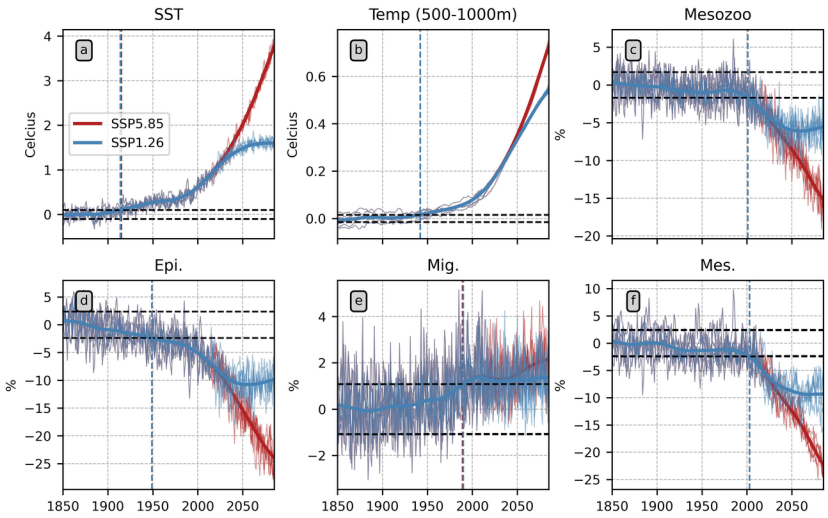

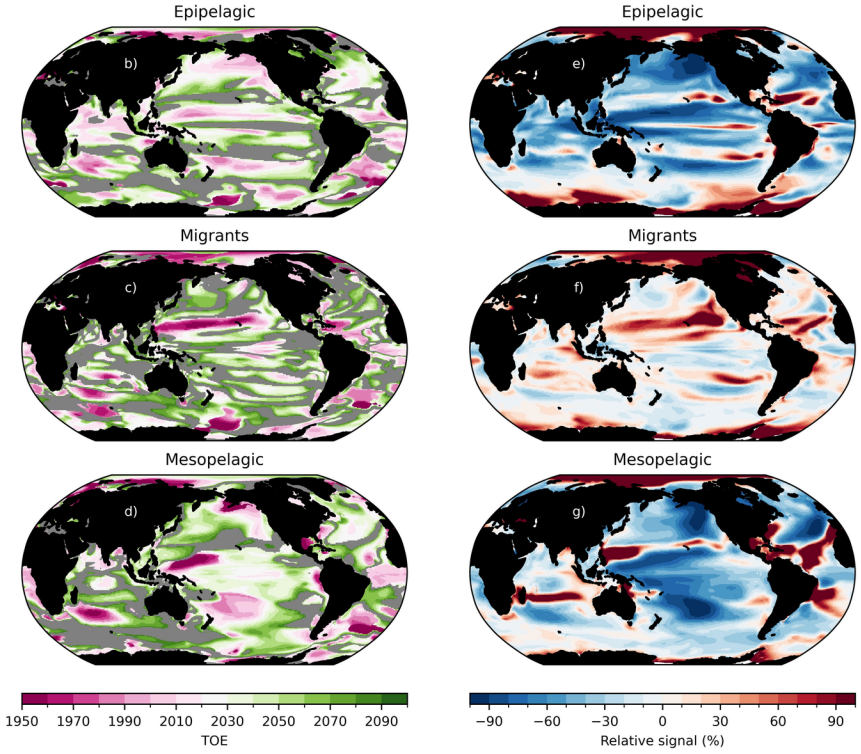

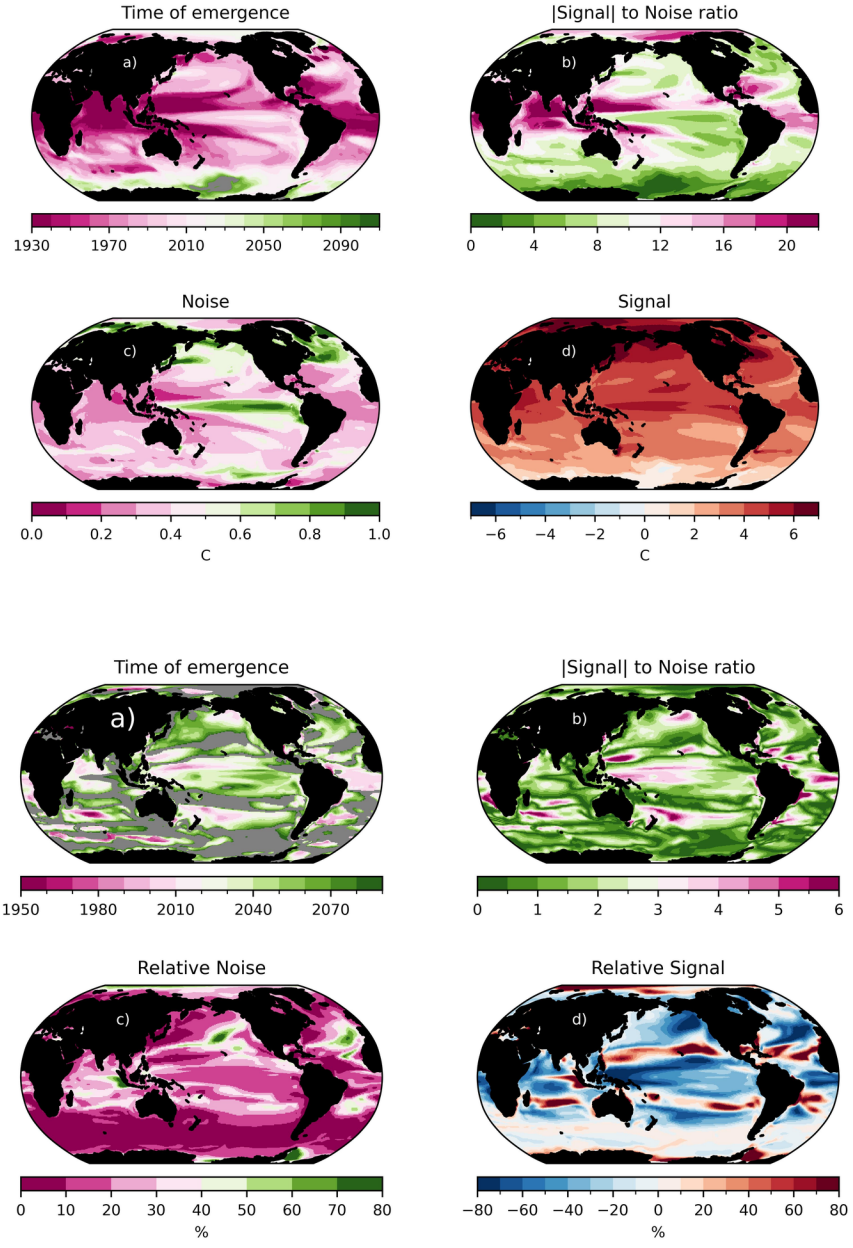

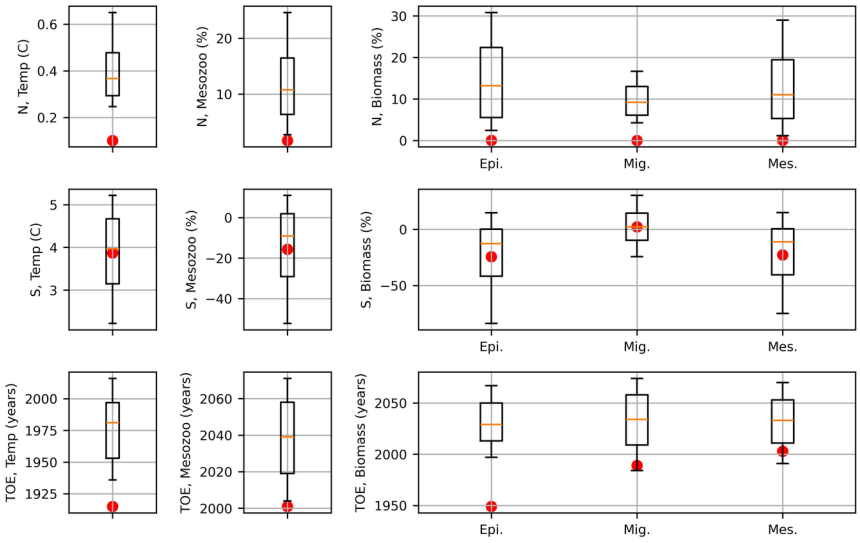

Assessing the time of emergence of global ocean fish biomass using ensemble climate to fish simulations

Nicolas Barrier[1*], Olivier Maury[1], Roland Seferian[2], Yeray Santana-Falcón[2], Matthieu Lengaigne[1]

[1]MARBEC, Univ. Montpellier, CNRS, Ifremer, IRD, Sète, France
[2]CNRM (Université de Toulouse, Météo-France, CNRS)

Key Points:

- The Time of Emergence (ToE) of marine ecosystem is investigated for the first time using ensemble climate-to-fish simulations
- Emergence of fish biomass is driven by the concentration of lower trophic levels and modulated by temperature through trophic amplification
- The ToE pattern closely follow the signal-to-noise ratio, which is mostly influenced by the strength of the climate change signal

*IRD, Marbec

Corresponding author: Nicolas Barrier, nicolas.barrier@ird.fr

Abstract

Climate change is anticipated to considerably reduce global marine fish biomass, driving marine ecosystems into unprecedented states with no historical analogues. The Time of Emergence (ToE) marks the pivotal moment when climate conditions (i.e. signal) deviate from pre-industrial norms (i.e. noise). Leveraging ensemble climate-to-fish simulations, this study examines the ToE of epipelagic, migratory and mesopelagic fish biomass, alongside their main environmental drivers, for two contrasted climate-change scenarios.

Globally-averaged biomass signals emerge over the historical period. Epipelagic biomass decline emerges earlier (1950) than mesozooplankton decline (2000) due to a stronger signal in the early 20th century, possibly related to trophic amplification induced by an early-emerging surface warming (1915). Trophic amplification is delayed for mesopelagic biomass due to postponed warming in the mesopelagic zone, resulting in a later emergence (2000). ToE displays strong size class dependence, with medium sizes (20 cm) experiencing delays compared to the largest (1 m) and smallest (1 cm) categories.

Regional signal emergence lags behind the global average, with median ToE estimates of 2029, 2034 and 2033 for epipelagic, mesopelagic and migrant communities, respectively, due to systematically larger local noise compared to global one. These ToEs are also spatially heterogeneous, driven predominantly by the signal pattern, akin to mesozooplankton. Additionally, our findings underscore that mitigation efforts (i.e. transitioning from SSP5-8.5 to SSP1-2.6 scenario) have a potential to curtail emerging ocean surface signals by 40%.

Plain Language Summary

Climate change is expected to have a significant impact on global marine fish biomass, leading marine ecosystems into unprecedented states. The Time of Emergence (ToE) is the moment when such a shift occurs. This study investigates the ToE of marine fish biomass is investigated using climate-to-fish simulations. Our results suggest that the emergence of global mean fish biomass occurs in the historical period (before 2020) and is controlled by small-size organisms (mesozooplankton) through food availability. We also show that the ToE strongly is highly dependent on organism size and varies regionally. Furthermore, we demonstrate that implementing mitigation policies significantly reduces the ar-

eas in which marine ecosystems emerge, thereby limiting the potential negative impacts of climate change.

1 Introduction

Anthropogenic climate change is expected to significantly impact the abundance and spatial distribution of pelagic communities of high trophic level organisms (HTL) (Lefort et al., 2015; Lotze et al., 2019; Tittensor et al., 2021). These impacts on HTLs arise from a myriad of climate-related stressors encompassing changes in lower trophic level organisms (LTL, i.e. microzooplankton, mesozooplankton), temperature, oxygen concentration, pH and ocean currents (Bijma et al., 2013; Bopp et al., 2013). Yet, the foremost pivotal factors driving these changes remain changes in temperature and primary production (Pörtner & Peck, 2011; Heneghan et al., 2021). Ocean warming, in particular, is indeed expected to accelerate metabolic rates and thus energy dissipation. In addition, temperature changes can affect the food consumption of organisms in different ways depending on the available food concentration (Guiet et al., 2016), resulting in a complex and diverse ecosystem response to temperature changes. In general, these changes are anticipated to potentially reduce HTL biomass for a given level of primary production (Heneghan et al., 2019). Moreover, ocean temperature changes is anticipated to cause a global decline in primary production (Pörtner et al., 2022), notably through increased stratification, which reduces nutrient concentrations in the euphotic zone. This will induce a global decline in LTL organisms, which are the fundamental energy source fuelling marine ecosystems (Chavez et al., 2011), and in turn a marked decrease in fish biomass. Given the importance of marine resources for both food security and the global economy, it is imperative to identify when and where these climate-induced impacts will exceed the natural variations of the marine ecosystems.

The Time of Emergence (ToE), as defined by Hawkins and Sutton (2012), represents the moment when a climate change signal becomes distinguishable from the inherent natural variability. ToE is typically identified when the ratio of anthropogenic signal (S) to natural climate noise (N), expressed as SNR, permanently exceeds a predetermined threshold (as seen in studies such as Giorgi and Bi (2009)). Historically conceived to assess when local climates deviate from their historical norms, ToE analysis holds particular relevance for ecosystems with limited adaptive capacity (Beaumont et al., 2011; Deutsch et al., 2008). Originally applied to terrestrial areas (Giorgi & Bi, 2009;

Diffenbaugh & Scherer, 2011), this concept has been extended to analyse changes in key environmental drivers of marine ecosystems, encompassing physical (Ying et al., 2022; Gopika et al., In prep; Santana-Falcón & Séférian, 2022) and biogeochemical variables (Keller et al., 2014; Rodgers et al., 2015; Henson et al., 2017). Earth System Model projections consistently indicate early emergence of sea surface temperature (SST) signals and much later emergence in primary production (Keller et al., 2014; Rodgers et al., 2015; Henson et al., 2017; Schlunegger et al., 2020). However, the ToE concept has not yet been applied to pelagic ecosystems projections.

Marine ecosystem models (MEMs) have been pivotal in projecting and understanding the impacts of climate change on marine ecosystems, notably through initiatives such as the Fisheries and Marine Ecosystem Model Intercomparison Project (FishMIP, Tittensor et al. (2018); Lotze et al. (2019); Tittensor et al. (2021)). On average, these projections indicate a reduction in global fish biomass at the end of the century of around 15-20% in a high emissions scenario (SSP5-8.5), and of around 5-7% in a low emissions scenario (SSP1-2.6) Lotze et al. (2019); Tittensor et al. (2021)). In addition, these studies highlight a spatial heterogeneity in the fish biomass response to climate change, hitting at potential increases in the Arctic Ocean and South Polar region while predicting decline elsewhere.

The primary objective of this study is to implement the ToE concept within projections generated by a global-scale marine ecosystem model, examining and contrasting these ToE with the pivotal environmental variables driving this model. Using the mechanistic ecosystem model APECOSM forced by ensemble simulations from the IPSL-CM6A-LR Earth System Model, for two contrasted emission scenarios(SSP5-8.5 and SSP1-2.6), we will first show that, when considering global average, the ToE is very early for the epipelagic (1950) and slightly later for the migratory and mesopelagic fish biomass (around 2000), with a strong dependency to the size class considered. Next, we show that the ToE at regional scale is considerably later than the globally averaged one, with strong dependency to the region and community considered. The paper is structured as follows. Section 2 describes the ecosystem and climate models, the simulation protocol and the methodology used to calculate the ToEs. Section 3 compares the ToEs estimated for the main ecosystem drivers, namely ocean temperature and mesozooplankton concentration, with those estimated for fish biomass. Summary and discussion are provided in 4.

2 Data and method

2.1 Marine ecosystem model

This study uses the Apex Predators ECOSystem Model (APECOSM, Maury et al. (2007); Maury (2010)) to simulate changes in marine fish biomass in the global ocean. APECOSM is a Eulerian ecosystem model that mechanistically represents the three-dimensional dynamics of size-structured pelagic populations and communities. It integrates individual, population and community levels and includes the effects of life-history diversity with a trait-based approach (Maury & Poggiale, 2013). Energy uptake and use for individual growth, development, reproduction, somatic and maturity maintenance are modelled according to the Dynamic Energy Budget (DEB) theory (Koojman, 2010), with metabolic rates dependent on both food and temperature.

APECOSM also includes important ecological processes such as opportunistic size-structured trophic interactions and competition for food, predatory, disease, ageing and starvation mortality, key physiological aspects such as vision and respiration, as well as essential processes such as three-dimensional passive transport by marine currents and active habitat-based movements (Faugeras & Maury, 2005), schooling and swarming (see Maury et al. (2007); Maury and Poggiale (2013); Maury (2017)).

In this study, we used the same APECOSM configuration as in Barrier et al. (2023), in which the model was used to analyse the ENSO-related variability of the biomass of epipelagic fish in the tropical Pacific Ocean. Three generic communities are simulated:

- The epipelagic community, which includes the organisms inhabiting surface waters during both day and night. Its vertical distribution is influenced by light and visible food during the day as well as temperature and oxygen during both day and night, while its functional response to prey is influenced by light and temperature.
- The migratory mesopelagic community, which includes organisms that feed at night in the surface layer and move to deeper waters during the day. Its vertical distribution is influenced by light during both day and night and visible food during the night.

- The resident mesopelagic community, which includes organisms that remain at depth during both day and night. Its vertical distribution is influenced by light and visible food during the day.

A more detailed description of this 3 community configuration is provided in (Barrier et al., 2023), in addition to a more thorough description of the model.

2.2 Climate model

In this study, APECOSM is forced by 3D physical (temperature, ocean currents) and biogeochemical (diatoms, microzooplankton, mesozooplankton, organic detritus, oxygen, light) outputs of the IPSL-CM6A-LR Boucher et al. (2020)) Earth System Model (ESM). This ESM has recently been used by the Fisheries and Marine Ecosystem Model Intercomparison Project (FishMIP) to assess the impacts of climate change on marine ecosystems, e.g. (Tittensor et al., 2021).

2.3 APECOSM Simulation protocol

The APECOSM simulation protocol used in this study is in agreement with the CMIP6 standards (Eyring et al., 2016). We therefore employ the same naming conventions.

First, a 100-year spin-up simulation has been performed using the outputs of the *piControl-spinup* ESM simulation, starting from a uniform biomass distribution of $1^{-34} J.m^{-2}.kg^{-1}$ for each community and size class. The end of the spin-up simulation is then used as a restart to run a pre-industrial simulation, using the outputs from the *piControl* climate simulation. The latter simulation was integrated for 500 years (1850-2349). Preindustrial CO_2 concentrations are prescribed in both the *piControl-spinup* and *piControl* climate simulations.

Next, 6 members of the *historical* simulations have been run using specific years of the *piControl* simulation as initial state. These years are chosen to ensure consistency with the climate simulations. The *historical* climate simulations cover the period from 1850 to 2014 and are constrained by observed annual greenhouse gas emissions. Finally, the end of the 6 *historical* simulation members have been used as initial states for the corresponding climate change simulations under the SSP5-8.5 and SSP1-2.6 "Shared So-

Simulation	Initial conditions	Simulation period
piControl-spinup	Uniform biomass distribution	1750-1850
piControl	*piControl-spinup*	1850-2349
hist-r1	*piControl* (1909-12-31)	1850-2014
hist-r2	*piControl* (1869-12-31)	1850-2014
hist-r3	*piControl* (1929-12-31)	1850-2014
hist-r4	*piControl* (1949-12-31)	1850-2014
hist-r6	*piControl* (2029-12-31)	1850-2014
hist-r14	*piControl* (1969-12-31)	1850-2014
ssp-r1	*hist-r1*	2015-2100
ssp-r2	*hist-r2*	2015-2100
ssp-r3	*hist-r3*	2015-2100
ssp-r4	*hist-r4*	2015-2100
ssp-r6	*hist-r6*	2015-2100
ssp-r14	*hist-r14*	2015-2100

Table 1. Simulations performed with the APECOSM model. The middle column indicates the initial condition used. If no date is provided, the end of the simulation is used.

cioeconomic Pathways" scenarios. These two scenarios represent the upper and lower ends of the CMIP6 future forcing pathways in the Integrated Assessment Modeling literature. SSP5-8.5 updates the CMIP5 RCP8.5 pathway and is the only SSP scenario with emissions high enough to produce a radiative forcing of 8.5 $W.m^{-2}$ in 2100 (O'Neill et al., 2016). SSP1-2.6 updates the CMIP5 RCP2.6 pathway and is anticipated to produce a multi-model mean of significantly less than 2°C warming by 2100 (O'Neill et al., 2016).

All the simulations are summarised in Table 1. It should be noted that the limited number of members used in this study is constrained by the availability of the biogeochemical variables in the IPSL-CM6-LR climate change scenarios.

2.4 Time of Emergence

As discussed in the introduction, ToE typically marks the moment when the ratio of anthropogenic signal (S) to natural climate noise (N), SNR, permanently exceeds

a predefined threshold (Giorgi & Bi, 2009). In this section, we illustrate the presentation of the methodology used to calculate the signal S, the noise N and the ToE using time series of global mean epipelagic fish biomass.

The methodology employed in (Hawkins & Sutton, 2012) for signal estimation, which assumes a proportional scaling between local changes and global variations, cannot be applied in our context. While this assumption holds true at first order for SST, it does not hold for biogeochemical and biological variables, whose climate change signal shows strong spatial and temporal heterogeneity (Lotze et al., 2019; Tittensor et al., 2021). Rather, the climate change signal in our approach is derived by averaging the historical and scenario time series over the 6 members, as shown in Fig. 1a (thin black curve). Since these members share identical external forcings and differ only in their initial state, the multi-member average serves as a good first approximation of the climate change signal. However, residual noise persists due to the limited number of available members. To remove this noise, a Gaussian filter with a standard deviation of 15 years is applied to smooth the multi-member mean (Fig. 1b). The resulting smoothed time series (thick black curve in Fig. 1a) is regarded as the climate change signal S.

Natural variability is then estimated by removing this climate change signal from each member time series. The resulting time series (Fig. 1c) represent the anomalies in fish biomass due solely to high-frequency climate and ecosystem variability. The noise N is then estimated by calculating the standard deviation of the anomalies over the time and member dimensions (black dashed curve in Fig. 1c).

Finally, we define ToE as the year when the climate change signal permanently exceeds the envelope of natural variability (black dashed curve in Fig. 1d), which we define as the historical multi-member mean computed between 1850 and 1900 plus or minus the standard deviation of the anomalies (N, Fig. 1d). To avoid potential artefacts due to truncation of the Gaussian smoothing kernel used to extract the signal, we consider that there is no emergence if the estimated ToE is later than 2085.

ToEs are calculated both globally and at each grid cell for temperature at the surface and averaged between 500 and 1000 m, surface mesozooplankton concentrations, and for the vertically integrated fish biomass density of each community and each size class. In addition, total fish biomass (i.e. biomass integrated over the entire size range) is also evaluated for each community.

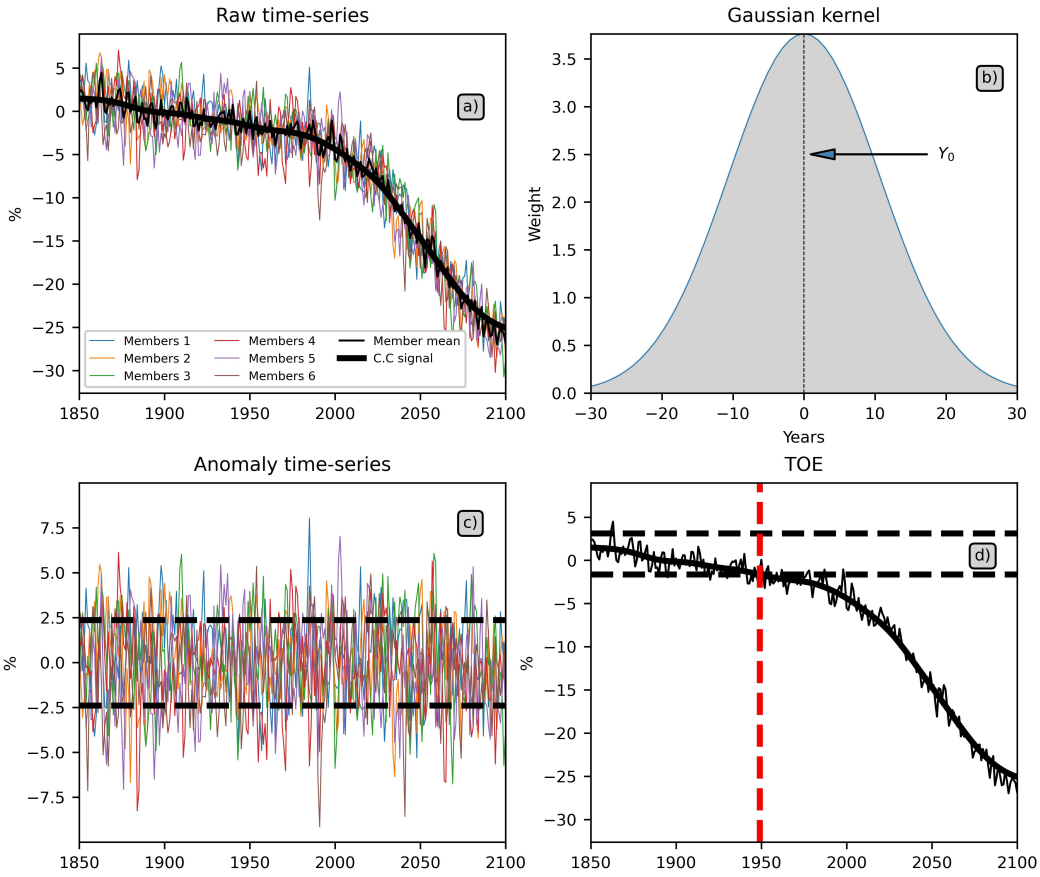

Figure 1. Overview of steps for calculating the time of emergence. Displayed is the time series for global mean epipelagic fish biomass. (a) Single-member time series (coloured lines), multi-member mean (thin black line) and climate change signal (thick black line). (b) Gaussian kernel illustration used to smooth the multi-member mean. (c) Computed noise obtained by subtracting the climate change signal from the original time series. These anomalies represent the range of natural variability (dashed lines). (d) Calculation of the time of emergence (dashed red line) as the moment when the climate change signal is permanently outside the range of natural variability.

3 Results

In this section, we first discuss the ToE for global mean temperature at the surface and between 500-1000 m, surface mesozooplankton concentrations and global mean total biomass for each community. Next, we investigate the ToE of mean fish biomass as a function of size. Finally, ToE computed from global mean time series is compared to the ToE computed on regional scales and the spatial patterns of ToE are described.

3.1 Global mean ToE

3.1.1 Environmental drivers and total fish biomass

Fig. 2 shows the global mean anomalies of temperature at the surface (SST) and averaged between 500 and 1000 m, surface mesozooplankton concentrations and fish biomass density (integrated between 0-1000m) of each community relative to the 1850-1900 period. The global mean SST starts increasing from 1900. This warming notably accelerates from 2000 onwards in the SSP5-8.5 scenario (red curve), exceeding 3.5° by the end of the 21st century (Fig. 2a) with respect to pre-industrial conditions. Conversely, in the SSP1-2.6 scenario, the warming reaches a plateau from the middle of the century (around 1.5°). Because of minimal noise attributable to the global average, SST emerges very early (1915) in both scenarios. The warming between 500 and 1000 m is weaker than that of the SST and starts later, resulting in a delayed emergence (around 1945).

Global surface mesozooplankton anomalies exhibit a strikingly similar low-frequency evolution in both scenarios (Fig. 2c), opposing that of temperature anomalies. They indeed show a pronounced decline starting at the turn of the 21st century. This reduction persists almost linearly until the century's end for the SSP5-8.5 scenario, reaching -15%. Conversely, in the SSP1-2.6 scenario, this decline moderates, with a relative decrease plateauing at -5% by the mid-century mark in 2050. Because of a weaker signal-to-noise ratio compared to temperature, the climate change signal for mesozooplankton emerges later (2001) compared to SST (1915).

Epipelagic fish biomass evolution mirrors that of mesozooplankton, suggesting a bottom-up control mechanism. However, by the end of the 21st century, the relative decline in epipelagic biomass surpasses that of mesozooplankton for both the SSP5-8.5 and SSP1-2.6 scenario, with reductions of 25% and 10% respectively for epipelagic biomass

compared to -15% and -5% for mesozooplankton. This heightened decline in epipelagic biomass is likely linked to trophic amplification, potentially driven by warmer temperatures, as discussed in de Luzinais et al. (2023). Furthermore, the epipelagic decline outpaces that of mesozooplankton throughout the 20th century, presumably for the same reason. This trophic amplification leads to an early emergence of global mean epipelagic biomass (1949).

Mesopelagic biomass evolution closely follows that of epipelagic biomass in terms of both timing and amplitude. Despite exhibiting a larger relative amplitude, it also mirrors the evolution of mesozooplankton and detritus concentrations (not shown), their primary food source, further suggesting a bottom-up control mechanism likely intensified by trophic amplification. However, although the relative noise of global mesopelagic and epipelagic biomass is similar (around 2%), the former declines more slowly than the latter, which results in a later emergence of mesopelagic fish (2001). This milder decrease could be attributed to a weaker trophic amplification during the early stages of the industrial era. Initially, the warming primarily affects the surface and gradually penetrates in deeper layers, resulting in a delayed warming effect in the mesopelagic zone and consequently in a less pronounced trophic amplification during the initial period. The trophic amplification gradually intensifies as surface warming signals penetrate deeper into the ocean over time (Fig. 2a and b).

In comparison to epipelagic and mesopelagic communities, global biomass changes of the migratory community is considerably weaker in 2100, increasing of +2% in the SSP5-8.5 scenario and 1% in the SSP1-2.6 scenario. Identifying a plausible mechanism driving these changes is more challenging than for the other communities, as the evolution of migratory biomass does not align with any of the predominant environmental drivers. Nonetheless, these changes emerge around the same time frame (1990) than those simulated for the mesopelagic community (2001), primarily because the weaker noise in the migratory (N of 1.07%) compared to the mesopelagic community (N of 2.35%) compensates for the weaker signal simulated at the turn of the 20th century (S of 2.32% and -25.56%, respectively).

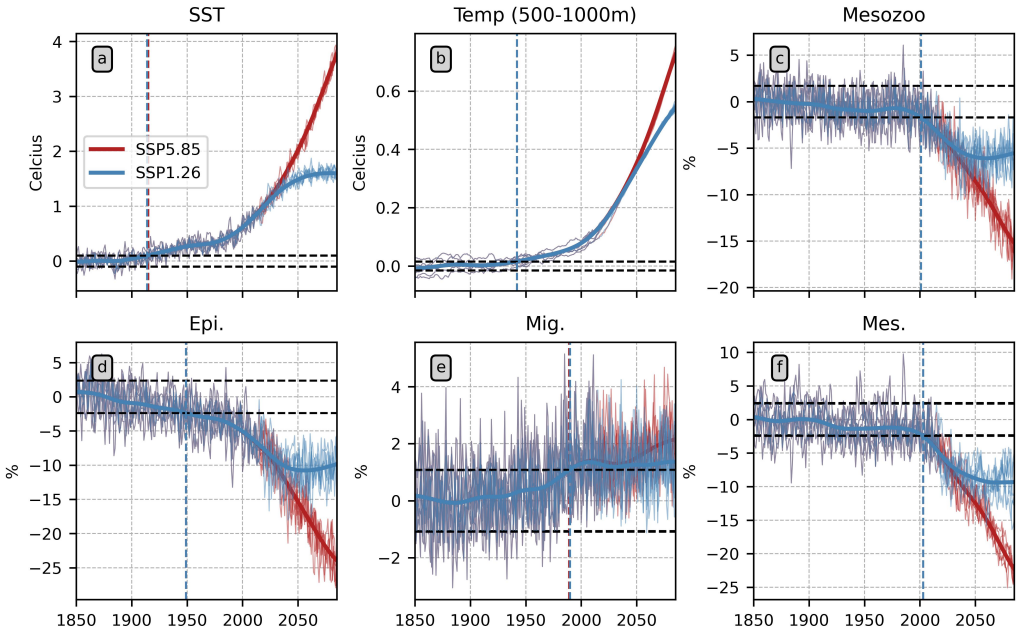

Figure 2. Global mean anomalies of temperature at the surface (a) and averaged between 500 and 1000 m (b), relative surface mesozooplankton concentrations (c) and global mean fish biomass for the epipelagic, migratory and mesopelagic communities (d-e-f). The thin lines represent the individual members, and the thick lines represent the climate change signal.

3.1.2 Sensitivity to the size class

As discussed for example in (Barrier et al., 2023), the response of marine fish biomass to changes in environmental drivers is size dependent. Consequently, the natural variability N, the climate change signal S and, hence, the ToE of fish biomass are expected to vary with size.

Fig. 3 allows examining the ToE sensitivity to the organisms size class for each community and the primary factor governing this sensitivity, whether it is noise or signal. We present only the results for the SSP5-8.5 scenario as they are insensitive to the scenario considered. The upper panels show the ToE as a function of size for each community, while lower panels illustrate the signal-to-noise ratio (SNR), the relative signal (S) and the relative noise (N). The ToE is early (1950) and stable for size classes smaller than 1 cm (Fig. 3a) and then increases from 1950 to 2000 for sizes ranging from 1 cm to 15 cm. This increase can be directly related to an increase in the noise within this size range (Fig. 3j), resulting in a weaker SNR (Fig. 3d) and therefore a delayed emergence. For

sizes exceeding 15 cm, the ToE experiences a steep decline, with the largest organisms (1 m) reaching an emergence date of 1920. This decline can predominantly be attributed to a signal increase within this size range (Fig. 3g).

The ToE for the mesopelagic varies with size in a similar way to the epipelagic community, reaching a maximum near 25 cm, albeit for different reasons. For the mesopelagic community, the SNR (Fig. 3f), and consequently the ToE (Fig. 3c), are primarily driven by the signal (Fig. 3i), which decreases up to 25 cm and then increases.

In contrast to epipelagic and mesopelagic communities, the signal of the migratory community (Fig. 3b) does not emerge for all size classes, with no signal emerging between 5 and 15 cm. This absence of emergence for intermediate size classes is attributed to a change in signal sign for 10 cm organisms (Fig. 3e), leading to a negligible SNR around this size class. In addition, the noise increase also contributes to the ToE increase for sizes smaller than 20 cm 3h).

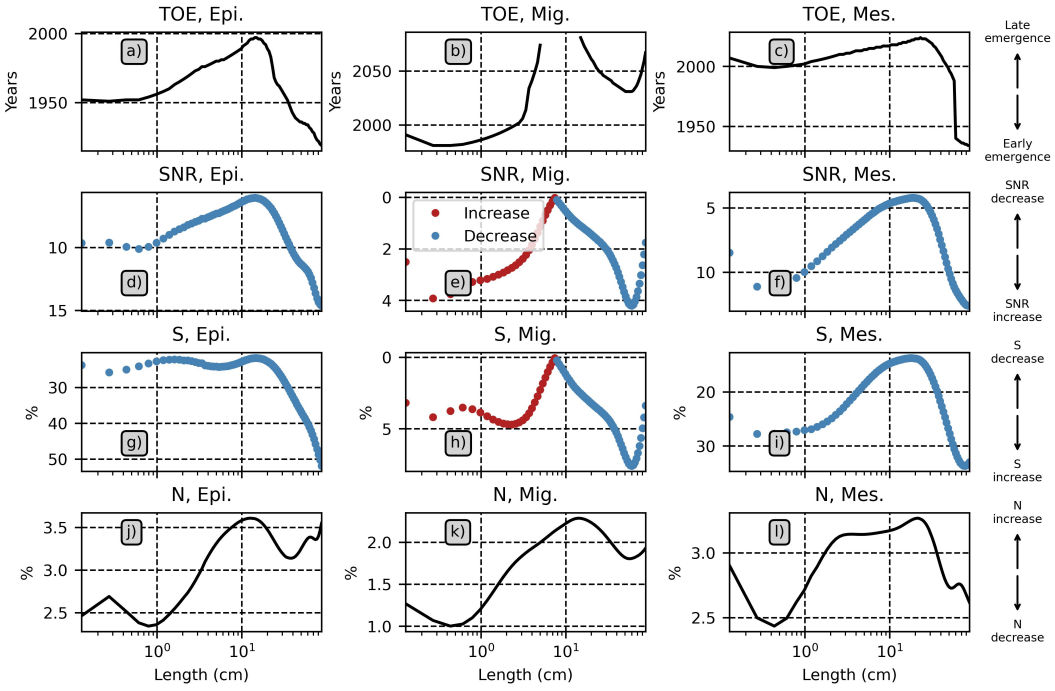

Figure 3. Time of emergence (a-c), signal to noise (d-f) ratio, relative signal (g-i) and relative noise (j-l) for epipelagic (left), migratory (middle) and mesopelagic (right) communities. In the second and third rows, biomass increase and decrease are depicted by red and blue dots, respectively. The y-axis are ordered in a way to facilitate the interpretation of the results.

297 ## 3.2 Regional ToE

298 ### *3.2.1 Comparison with global mean ToE*

299 The previous subsection demonstrates that, when globally averaged, fish biomass
300 signals emerge early, mostly during the historical period. This result is likely to be re-
301 lated to a significant reduction in noise through spatial averaging, leading to an increase
302 in SNR. In this subsection, the ToE calculated at regional scale (at grid scale) is com-
303 pared to the ToE of global mean time series. As the findings remain consistent across
304 the two scenarios considered, we focus on the SSP5-8.5 scenario.

305 Fig. 4 shows the percentage of the ocean surface where a signal emerges each decade
306 (vertical bars) alongside the cumulative surface where a signal has emerged over time
307 (continuous line). Regional SSTs exhibit early regional emergence, starting between 1920
308 and 1930 and peaking between 1970 and 1990. In terms of cumulative percentage, SST
309 signals have emerged over about 90% of the ocean surface by 2020, reaching 97% by the
310 end of the century. In contrast, regional mesozooplankton biomass start emerging much
311 later, around 1970, and peak in 2030. By 2020, mesozooplankton has emerged over only
312 23% of the ocean surface, gradually increasing to 64% by the end of the century. This
313 corresponds to a time lag of approximately 50 years between the regional ToE for meso-
314 zooplankton and SST.

315 The timing of regional emergence for total fish biomass is comparable for all three
316 communities, with the mesopelagic and migratory communities emerging slightly before
317 the epipelagic community. Consequently, the percentages of the ocean surface showing
318 emergence are qualitatively similar between communities, ranging from 28% to 36% by
319 2020 and 64 to 75% by 2100. The timing of emergence for regional fish biomass is sim-
320 ilar to that of mesozooplankton (purple curve) but about a decade earlier, especially for
321 epipelagic organisms, confirming both the bottom-up influence of lower trophic levels on
322 higher trophic levels and the trophic amplification phenomenon already discussed for global
323 scale (Fig. 2).

324 For all variables considered here, the peaks of regional emergence occur later than
325 the emergence of the global mean time series. For example, the peak of regional SST emer-
326 gence occurs 60 years later than the emergence of the global mean SST, while the lag

is of about 30 years for mesozooplankton, 75 years for epipelagic and 35 years for migratory and mesopelagic fish communities (dashed lines in Fig. 4).

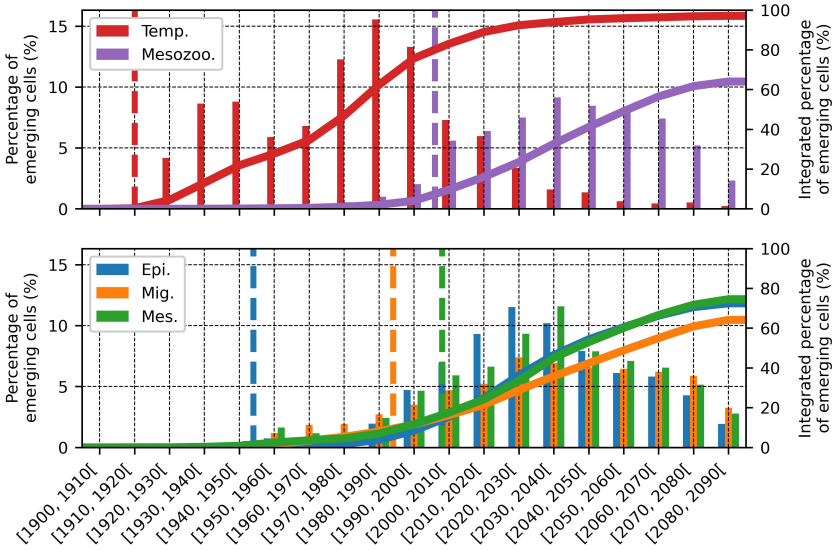

Figure 4. Percentage of the ocean surface where a signal has emerged at grid scale during a given decade (x-axis) for SST (red bars) mesozooplankton concentration at the surface (purple bars), biomass of the epipelagic fish community (blue), mesopelagic migratory fish community (orange), mesopelagic resident fish community (green). The continuous lines show the corresponding cumulative percentages. The dashed vertical lines indicate the ToE of global mean time-series.

Fig. 5 compares the 10^{th}, 25^{th}, 50^{th} (median), 75^{th} and 90^{th} percentiles of the local noise N (upper panels), signal S (middle panels) and ToE (lower panels) distributions with the values obtained from the global mean time series (red dots). In all cases, the noise values for global averages are either smaller or close to the 10^{th} percentile of the local noise. Conversely, the global mean signal aligns more closely to the signal calculated locally, falling between the 25^{th} and 75^{th} percentiles for all variables. Consequently, due to this considerably weaker noise and relatively consistent signal at global scale, global ToE precedes that of local ones. For example, the ToE for global mean SST, mesozooplankton and epipelagic fish biomass lies below the 10^{th} percentile of the local ToE, while it ranges between the 10^{th} and the 25^{th} percentiles for migratory and mesopelagic fish biomass.

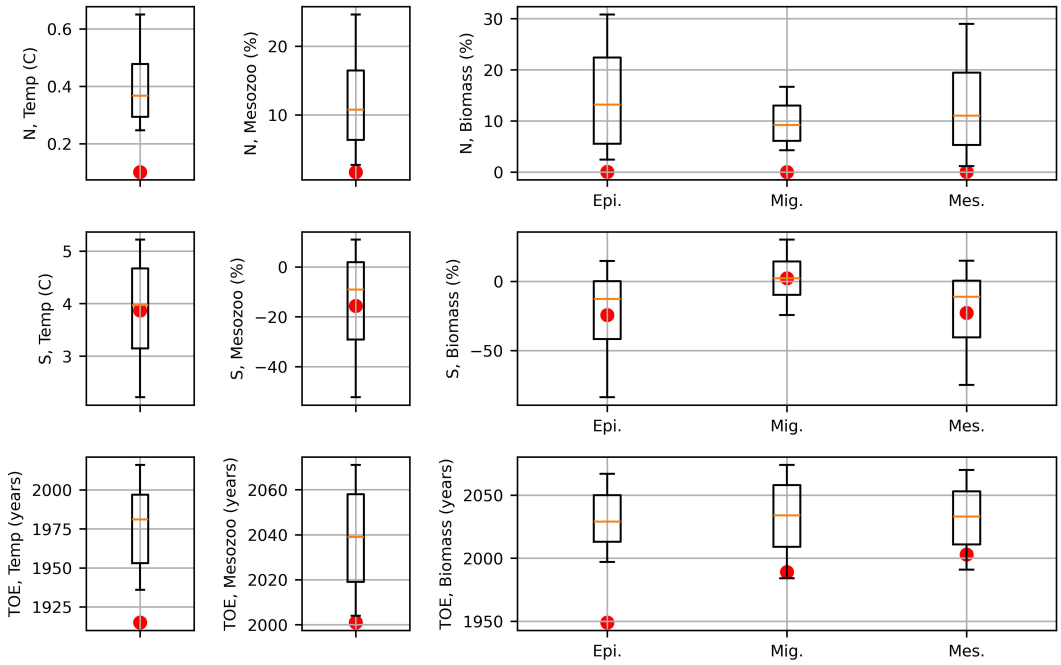

Figure 5. Whisker plot showing the 10^{th}, 25^{th}, 50^{th} 75^{th} and 90^{th} percentiles of spatial noise, signal and time of emergence for sea surface temperature, surface mesozooplankton and fish biomass. Red dots indicate the values obtained from the global time series. Mesozooplankton and fish biomass noise and signal are represented in anomalies relative to the historical (1850-1950) global mean value.

3.2.2 Spatial patterns

In the following, the spatial patterns of ToE for SST, surface mesozooplankton and total fish biomass per community are analysed. The focus is laid on the SSP5-8.5 scenario, where over 60% of the ocean surface exhibits emergence at the end of the century for all biological variables.

Sea surface temperature

Fig. 6a shows the ToE map for SST. As expected from Fig. 4, most of the oceanic regions emerge early. In particular, the earliest emergence occurs in the tropical Indian Ocean, the tropical Atlantic and the Western Pacific. However, several areas exhibit a late emergence, such as the eastern equatorial Pacific, which manifests emergence around 2010, along with mid-latitude regions and Antarctica. These patterns are consistent with

findings from previous studies derived from other ESMs (see for instance Fig. 4 of Schlunegger et al. (2020)).

Fig. 6b shows the SNR map for SST, which is closely related to ToE. Here, the noise (Fig. 6c) is defined as the standard deviation of the anomalies relative to the climate change signal (see section 2.4), and the signal (Fig 6d) is defined as the difference between the SSP5-8.5 multi-member mean SST averaged between 2070 and 2100 and the historical multi-member SST averaged between 1850 and 1900. The SNR pattern mirrors the ToE map, indicating an early emergence in regions with a large SNR ratio and a late emergence in areas with a smaller ratio. The SST signal (Fig. 6d) shows much less spatial variation than the noise (Fig. 6c) and the SNR is predominantly influenced by the noise, with a spatial correlation between the SNR and the inverse of the noise reaching 0.71. In particular, the large noise and hence the late emergence of SST in the tropical Pacific are related to the strong ENSO variability (Diaz et al., 2001). Similarly, in the North Pacific and the Atlantic oceans, delayed emergence arises from the large noise induced by the Pacific North American pattern and the North Atlantic Oscillation (Hurrell & Deser, 2009), respectively. The correlation of SNR with the signal is 0.47. In particular, the weak SNR and hence the late emergence of SST in the Southern Ocean is due to a weaker signal.

Surface mesozooplankton

As expected from Fig. 4, the ToE map for mesozooplankton shows broad regions where the signal has not emerged by the end of the century. Signals have emerged in most of the tropical ocean, with early emergence occurring in the equatorial Atlantic, western Pacific and western Indian Ocean. On the contrary, ToE patterns are more patchy and less homogeneous at mid and high latitudes, with early emergence in the subtropical Pacific gyres (2010) and no emergence on their flanks. Compared to the SST, the mesozooplankton signal displays very large spatial variations, from a strong decrease in the tropics, especially in the equatorial Atlantic and western Pacific, to a strong increase in the subtropical Pacific gyres. These regions with a prominent mesozooplankton response generally correspond to those with early emergence. In contrast to SST, the signal-to-noise ratio and hence the ToE for mesozooplankton is predominantly driven by the signal (spatial correlation of 0.59) rather than by the noise (spatial correlation with the inverse of the noise of -0.02). This is particularly true in regions where the signal-to-noise

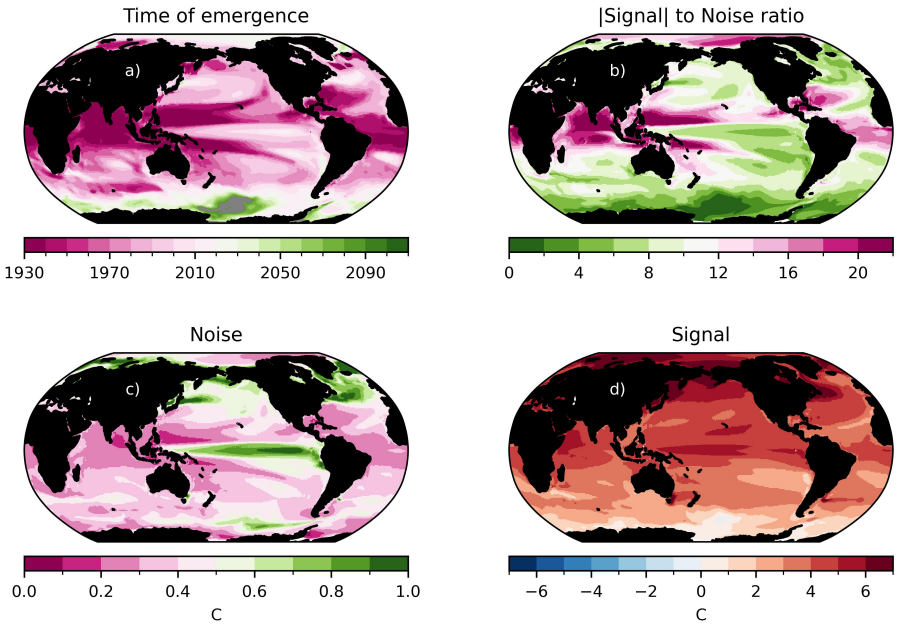

Figure 6. Maps of ToE (a), SNR (b), noise (c) and signal (d) for SST. Noise is calculated as the standard deviation of the anomalies relative to the climate change signal. Signal is calculated as the difference between the SSP585 temperature averaged over the 2070-2100 period and the historical temperature averaged between 1850 and 1900. In a), grey shadings indicate areas that have not emerged.

ratio is the highest (pink areas in Fig. 7b), which are associated with very strong signals (either positive or negative). These regions are also the earliest to emerge (before 2010).

Fish biomass

The SNR, and consequently the associated ToE, predominantly mirror the signal within the three communities, as illustrated in Fig. 8e, f and g. Areas exhibiting early emergence coincide with those displaying stronger signal, whether positive or negative. This visual assessment finds further support in the pattern correlation between the SNR and the relative signal, which reaches 0.76, 0.74 and 0.89 for the epipelagic, migratory and mesopelagic communities, respectively. Conversely, the correlation with the inverse of the relative noise is much lower (0.04, -0.06 and -0.004, respectively).

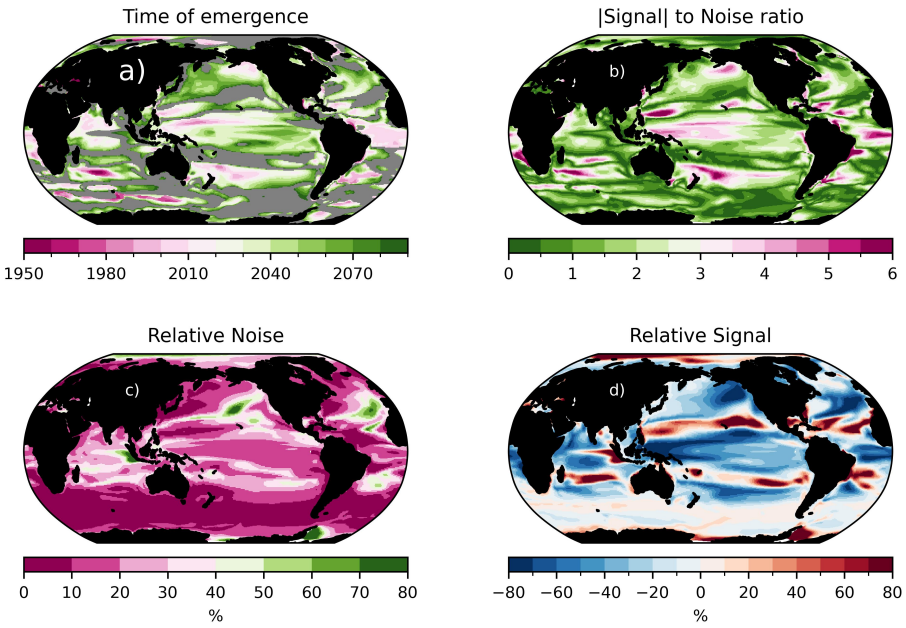

Figure 7. Time of emergence (a), signal-to-noise ratio (b), noise (c) and signal (d) for sea surface mesozooplankton concentration. The noise is given as the standard deviation of the anomalies relative to the climate change signal. The signal is provided as the difference between the SSP5-8.5 mesozooplankton averaged over the 2070-2100 period and the historical mesozooplankton averaged between 1850 and 1900. The latter is also used to normalise the standard deviation and signal, which are presented as percentages. In a), grey shading indicates areas that have not emerged.

Although the three communities display a similar emergence timeline at the global scale (Fig. 8a), the spatial patterns of their ToE show striking disparities, as illustrated in Fig. 8b-d. The epipelagic and resident communities emerge over wide regions (Fig. 8b,d), in contrast to the migratory community, which displays a more fragmented emergence pattern (Fig. 8c). This distinctive characteristics may be attributed to differences in the strength of signal among these communities. Both the epipelagic and mesopelagic communities (Fig. 8e,g) display a decline in fish biomass across most oceanic regions, which explains the strong decrease of global mean biomass (about -20%, Fig. 2d and f). On the other hand, the migratory community exhibits both increasing and decreasing signals at a regional scale (Fig. 8f), which explains the small increase (about +2%) of global mean migratory fish biomass (Fig. 2e).

The epipelagic fish biomass emerges before 2020 in various regions such as the tropical Pacific and Atlantic on both sides of the equator, the northern and southern Pacific and Atlantic Oceans and southeast of Madagascar (Fig. 8b). These regions of early emergence align with the early emergence of mesozooplankton biomass (Fig. 7a), which corresponds to a pronounced decline in mesozooplankton concentration (Fig. 7e) and epipelagic fish biomass (Fig. 7d). The projected patterns for the epipelagic community resemble those for mesozooplankton (pattern correlation of 0.61), indicating that changes in mesozooplankton concentration are the predominant drivers of projected changes in epipelagic fish biomass, as already inferred from global mean time series (Fig. 2). This influence is more substantial than that of temperature, which exhibits a much earlier emergence and distinctly different patterns (Fig 6d, pattern correlation of -0.00). Although not structuring the ToE spatial patterns for the epipelagic community, warmer temperatures likely induce early emergence (median value around 2025, Fig. 5), presumably through trophic amplification (de Luzinais et al., 2023).

Regarding the migratory community, the most striking feature is the very early emergence (around 1950) that occurs in the central Pacific, at about 15°N. This area of early emergence coincides with a strong positive mesozooplankton concentrations signal in the gyres (Fig. 7d), which in turn leads to a marked increase in the migratory fish biomass (Fig. 7f).

The mesopelagic community shows an emerging signal across extensive regions of the Pacific and Atlantic Oceans, particularly in areas characterised by moderate to pronounced mesopelagic biomass decline. Signals emerge before 2020 in specific areas, such as the north of the equatorial western Pacific, off New Zealand and around the Fiji Islands, as well as in the equatorial and South-West Atlantic and the south-western region of the Indian Ocean off the island of Madagascar. The projected patterns for the mesopelagic community (Fig. 8c) also demonstrate some resemblance to those of mesozooplankton (Fig. 7d, pattern correlation of 0.48), although to a lesser extent compared to the congruence observed in the epipelagic community. This discrepancy is likely related to the model representation, where mesopelagic organisms feed on the migratory community that inhabits mesopelagic waters during the day and on organic detritus, both of which exhibiting different horizontal distributions than mesozooplankton.

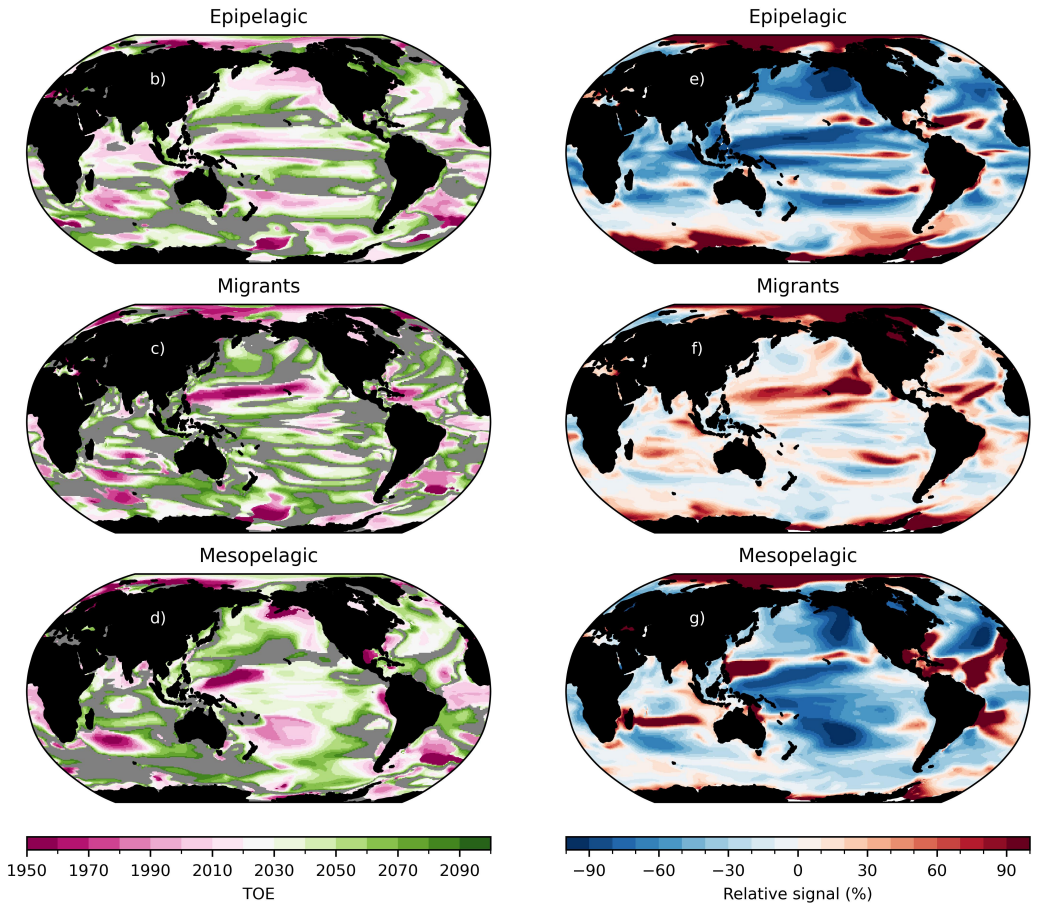

Figure 8. (a) Surface of the ocean in which the epipelagic, migratory and mesopelagic total fish biomass emerge in a given decade. The continuous lines show the cumulated percentage. The red and purple lines show the cumulative percentage for temperature and mesozooplankton (cf. Fig 4). (b-c-d) ToE maps for each of the three communities, with non emerging areas in gray. (e-f-g) Relative climate change signal for each of the three communities, computed as the difference between the SSP585 average over the 2070-2100 period and the *historical* average between 1850 and 1900. The latter is also used to normalise the signal and represent it as percentage.

4 Discussion and summary

4.1 Discussion

In the above, regional ToE patterns have been investigated for the SSP5-8.5 scenario, in which 60% of the ocean surface will emerge by the end of the century. We have also shown that global mean time series emerge during the historical period (before 2020). One question that arises is whether mitigation policies can reduce the regional emergence.

Fig. 9 compares the cumulative percentage of the emerging ocean surface for temperature, mesozooplankton and fish biomass climate change signal for both SSP5-8.5 and SSP1-2.6 scenarios. While the scenario has a marginal impact on the ToE of SST, with 93% of the ocean surface emerging by the end of the century in SSP1-2.6 (compared to 97% in SSP5-8.5), it significantly reduces the surface impacted by climate change compared to SSP5-8.5 for biological signals. By the end of the century, mesozooplankton emerges in 31% of the ocean in the SSP1-2.6 scenario compared to 64% in the SSP5-8.5 scenario. Similarly, epipelagic, migratory and mesopelagic fish biomass emerge in 41%, 38% and 49% of the ocean in the SSP126 scenario and in 72%, 64% and 75% in the SSP585 scenario. Therefore, while the emergence of global fish biomass occurs during the historical period (prior to 2020), mitigation policies can maintain future marine ecosystems within the range of their natural variations in most of the ocean's regions. These differences in the response of global mean and regional ToEs to mitigation are also a consequence of the weaker noise in the former. Considering global time series, the weaker signal of the SSP1-2.6 scenario is sufficient to exceed the range of natural variability, which is not the case when grid-scale ToEs are considered.

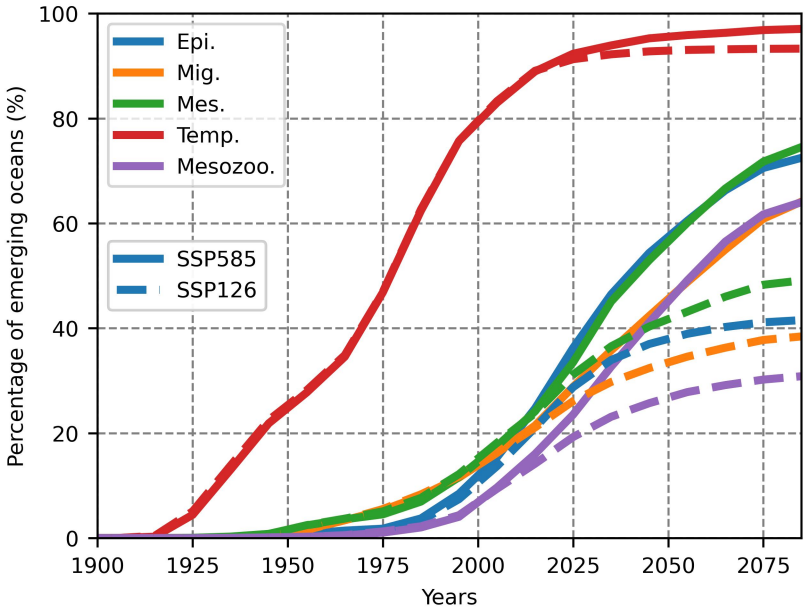

Figure 9. Cumulative percentage of the ocean surface in which the signal emerges for environmental variables and fish biomass in the SSP585 and the SSP126 scenarios

Our analysis also underscores the influence of the size class on the ToE. Notably, small (< 1 cm) and large (> 50 cm) epipelagic and mesopelagic organisms exhibits earlier emergence than their intermediate-sizes counterparts (about 20 cm). The later emergence of intermediate size organisms results from a larger noise within the epipelagic community and a weaker signal within the mesopelagic community. On the other hand, migratory fish of intermediate size fail to emerge due to a shift of their climate change signal from positive (for small sizes) to negative (for large sizes). While understanding the changes in natural variability and in the response to climate change with size is beyond the scope of this study, it presents a compelling avenue for future investigation. Potential approaches may involve decomposing biomass changes into their main contributions (predation, growth, advection, diffusion, Barrier et al. (2023)), or conducting sensitivity analyses akin to those performed in Heneghan et al. (2019).

Furthermore, previous literature highlighted the large persisting uncertainties regarding the climate change signal and ToE of biogeochemical variables. For example, using large ensembles from four Earth System Models (ESMs), Schlunegger et al. (2020) findings point to robust climate change signal and ToE for SST across four different ESMs ensemble but far less consistency for chlorophyll concentration and carbon export. Uncertainties in the climate change signal of biogeochemical processes are well known (e.g. Bopp et al. (2022)) and can lead to large uncertainties on the fish biomass response to climate change, especially when the biogeochemical models are driven by the primary production, which is more uncertain than the planktonic biomass (Tittensor et al., 2021). Although APECOSM uses plankton biomass, which is more sounded as a forcing variable, it is reasonable to anticipate large uncertainties on the ToE estimates for fish biomass. Another source of uncertainties stems from the limited number of members used in our study. Due to the limited availability of the biogeochemical forcing variables required to run APECOSM, stored from the IPSL-CM6-LR model, only 6 members could be considered, in comparison to the 30 members that were used in Schlunegger et al. (2020). Additionally, only one marine ecosystem model has been considered in this study. However, large uncertainties remain in the mechanisms driving the response of marine ecosystems to climate change Heneghan et al. (2019). One way to address these uncertainties would be to derive multi-model ensembles of ToE estimates from the ensemble simulations that have been carried out as part of the Fisheries and Marine Ecosystem Model Intercomparison Project (FishMIP, Tittensor et al. (2018); Lotze et al. (2019); Titten-

sor et al. (2021)), which includes 16 climate-to-fish simulations, with 9 ecosystem models forced by two different climate models.

Finally, we only considered the impact of climate change on the ecosystem. However, fishing also has a significant impact on fish biomass. For example, using data from the Pacific tuna fisheries, Sibert et al. (2006) have shown that the fish biomass of tunas larger than 175 cm declined by about 40% at the end of the 1970s due to longline fisheries. At the same time, purse-seine fishery began to affect smaller fish ($\approx$ 75 cm) in the 1980s. This decline in fish biomass due to fishing would superimpose on the decline due to climate change, inevitably affecting the estimated ToE of marine fish biomass. Recognising this, the FishMIP community has begun to develop a new socio-economic scenario framework derived from the SSPs, called Ocean System Pathways (the OSPs, Maury et al. (2024), this issue). The OSPs are designed to project the spatio-temporal dynamics of fisheries and marine ecosystems. Using this innovative scenario framework, it will be possible to explore the impact of both fisheries and climate change on the emergence of fish biomass changes, and to identify potential synergies between these factors. OSPs could be used to address the additive effects of fishing on the emergence of marine ecosystems.

4.2 Summary

This study represents the first attempt to estimate the Time of Emergence (ToE) of climate change driven in fish biomass changes. ToE refers to the moment when these changes have or will emerge from the natural background variability. Using ensemble climate to fish simulations based on the APECOSM ecosystem model forced with the IPSL-CM6-LR Earth System physical and biogeochemical outputs, we determine the ToE of the epipelagic, migratory and mesopelagic communities and their two main environmental drivers, temperature and mesozooplankton.

Globally averaged fish biomass signals emerge during the historical period across all three communities. The epipelagic and mesopelagic fish biomass decline mirrors that of mesozooplankton, suggesting a bottom-up control of their response to climate change. However, the signal of epipelagic fish biomass emerges earlier (1950) than that of mesozooplankton (2000) due to a stronger signal in the early 20th century, likely related to trophic amplification induced by an early emerging surface warming (1915). Conversely,

the trophic amplification for the mesopelagic community lags due to a delayed warming in the mesopelagic zone (500-1000 m), resulting in a later emergence (2000). While global migratory fish biomass also emerges during the historical period, its signal is considerably weaker than that of the other two communities.

Regional emergence lags behind that of global mean signals. For example, the peak of regional mesozooplankton emergence occurs 30 years later than that of the global mean mesozooplankton, 75 years for epipelagic and 35 years for migratory and mesopelagic fish communities. This delay can be tracked back to a considerably weaker globally-averaged noise compared to regional one. Consequently, mitigation policies could strongly reduce the ocean surface where biogeochemical and biological signals emerge (about 60% in the SSP5-8.5 scenario and about 30% in the SSP1-2.6 scenario).

Open Research Section

The APECOSM model is available here: `https://github.com/apecosm/apecosm-private`. Access will be provided on request to the corresponding author. The version used in this study is `c0a910b8`.

The APECOSM configuration files are available on Zenodo: `https://doi.org/10.5281/zenodo.10454379`

All the Python scripts used to analyse the results are available here: `https://github.com/barriern/stage-maelys`.

Acknowledgments

The authors acknowledge the World Climate Research Programme, which, through its Working Group on Coupled Modelling, coordinated and promoted CMIP6. We thank the climate modelling groups for producing and making available their model output, the Earth System Grid Federation (ESGF) for archiving the data and providing access, and the multiple funding agencies who support CMIP6 and ESGF.

The authors acknowledge the Pôle de Calcul et de Données Marines (PCDM, `http://www.ifremer.fr/pcdm`) for providing DATARMOR storage, data access, computation resources, visualisation and support services.

The authors acknowledge Maelys Metge, who started this work as part of her internship.

The authors acknowledge the support from the European Union's Horizon 2020 research and innovation program under grant agreement N° 817806 (TRIATLAS) as well as support from the French ANR project CIGOEF (grant ANR-17-CE32-0008-01).

The authors acknowledge DeepL Write (`https://www.deepl.com/write`), which was used to improve the English in the manuscript.

References

Barrier, N., Lengaigne, M., Rault, J., Person, R., Ethé, C., Aumont, O., & Maury, O. (2023, April). Mechanisms underlying the epipelagic ecosystem response to ENSO in the equatorial Pacific ocean. *Progress in Oceanography*, *213*, 103002. doi: 10.1016/j.pocean.2023.103002

Beaumont, L. J., Pitman, A., Perkins, S., Zimmermann, N. E., Yoccoz, N. G., & Thuiller, W. (2011, February). Impacts of climate change on the world's most exceptional ecoregions. *Proceedings of the National Academy of Sciences*, *108*(6), 2306–2311. doi: 10.1073/pnas.1007217108

Bijma, J., Pörtner, H.-O., Yesson, C., & Rogers, A. D. (2013, September). Climate change and the oceans – What does the future hold? *Marine Pollution Bulletin*, *74*(2), 495–505. doi: 10.1016/j.marpolbul.2013.07.022

Bopp, L., Aumont, O., Kwiatkowski, L., Clerc, C., Dupont, L., Ethé, C., ... Tagliabue, A. (2022, September). Diazotrophy as a key driver of the response of marine net primary productivity to climate change. *Biogeosciences*, *19*(17), 4267–4285. doi: 10.5194/bg-19-4267-2022

Bopp, L., Resplandy, L., Orr, J. C., Doney, S. C., Dunne, J. P., Gehlen, M., ... Vichi, M. (2013, October). Multiple stressors of ocean ecosystems in the 21st century: Projections with CMIP5 models. *Biogeosciences*, *10*(10), 6225–6245. doi: 10.5194/bg-10-6225-2013

Boucher, O., Servonnat, J., Albright, A. L., Aumont, O., Balkanski, Y., Bastrikov, V., ... Vuichard, N. (2020). Presentation and Evaluation of the IPSL-CM6A-LR Climate Model. *Journal of Advances in Modeling Earth Systems*, *12*(7), e2019MS002010. doi: 10.1029/2019MS002010

Chavez, F. P., Messié, M., & Pennington, J. T. (2011). Marine Primary Production in Relation to Climate Variability and Change. *Annual Review of Marine Science*, *3*, 227–260. doi: 10.1146/annurev.marine.010908.163917

de Luzinais, V. G., du Pontavice, H., Reygondeau, G., Barrier, N., Blanchard, J. L., Bornarel, V., ... Gascuel, D. (2023, August). Trophic amplification: A model intercomparison of climate driven changes in marine food webs. *PLOS ONE*, *18*(8), e0287570. doi: 10.1371/journal.pone.0287570

Deutsch, C. A., Tewksbury, J. J., Huey, R. B., Sheldon, K. S., Ghalambor, C. K., Haak, D. C., & Martin, P. R. (2008, May). Impacts of climate warming on terrestrial ectotherms across latitude. *Proceedings of the National Academy of Sciences*, *105*(18), 6668–6672. doi: 10.1073/pnas.0709472105

Diaz, H. F., Hoerling, M. P., & Eischeid, J. K. (2001). ENSO variability, teleconnections and climate change. *International Journal of Climatology*, *21*(15), 1845–1862. doi: 10.1002/joc.631

Diffenbaugh, N. S., & Scherer, M. (2011, August). Observational and model evidence of global emergence of permanent, unprecedented heat in the 20th and 21st centuries. *Climatic Change*, *107*(3), 615–624. doi: 10.1007/s10584-011-0112-y

Eyring, V., Bony, S., Meehl, G. A., Senior, C. A., Stevens, B., Stouffer, R. J., & Taylor, K. E. (2016, May). Overview of the Coupled Model Intercomparison Project Phase 6 (CMIP6) experimental design and organization. *Geoscientific Model Development*, *9*(5), 1937–1958. doi: 10.5194/gmd-9-1937-2016

Faugeras, B., & Maury, O. (2005). An advection-diffusion-reaction size-structured fish population dynamics model combined with a statistical parameter estimation procedure: Application to the Indian Ocean skipjack tuna fishery. *Mathematical Biosciences and Engineering*, *2*(4), 719. doi: 10.3934/mbe.2005.2.719

Giorgi, F., & Bi, X. (2009). Time of emergence (TOE) of GHG-forced precipitation change hot-spots. *Geophysical Research Letters*, *36*(6). doi: 10.1029/2009GL037593

Gopika, S., Lengaigne, M., Vialard, J., Izumo, T., Kwatra, S., Singh, N., & Suresh, I. (In prep). Time of Detection of Climate Change Sea Surface Temperature signals: CMIP vs. Observations. *Climate Dynamics*.

Guiet, J., Aumont, O., Poggiale, J.-C., & Maury, O. (2016, August). Effects of lower trophic level biomass and water temperature on fish communi-

ties: A modelling study. *Progress in Oceanography*, *146*, 22–37. doi: 10.1016/j.pocean.2016.04.003

Hawkins, E., & Sutton, R. (2012). Time of emergence of climate signals. *Geophysical Research Letters*, *39*(1). doi: 10.1029/2011GL050087

Heneghan, R. F., Galbraith, E., Blanchard, J. L., Harrison, C., Barrier, N., Bulman, C., ... Tittensor, D. P. (2021, November). Disentangling diverse responses to climate change among global marine ecosystem models. *Progress in Oceanography*, *198*, 102659. doi: 10.1016/j.pocean.2021.102659

Heneghan, R. F., Hatton, I. A., & Galbraith, E. D. (2019, May). Climate change impacts on marine ecosystems through the lens of the size spectrum. *Emerging Topics in Life Sciences*, *3*(2), 233–243. doi: 10.1042/ETLS20190042

Henson, S. A., Beaulieu, C., Ilyina, T., John, J. G., Long, M., Séférian, R., ... Sarmiento, J. L. (2017, March). Rapid emergence of climate change in environmental drivers of marine ecosystems. *Nature Communications*, *8*(1), 14682. doi: 10.1038/ncomms14682

Hurrell, J. W., & Deser, C. (2009, August). North Atlantic climate variability: The role of the North Atlantic Oscillation. *Journal of Marine Systems*, *78*(1), 28–41. doi: 10.1016/j.jmarsys.2008.11.026

Keller, K. M., Joos, F., & Raible, C. C. (2014, July). Time of emergence of trends in ocean biogeochemistry. *Biogeosciences*, *11*(13), 3647–3659. doi: 10.5194/bg-11-3647-2014

Koojman, S. (2010). *Dynamic Energy Budget theory for metabolic organisation* (Third ed.).

Lefort, S., Aumont, O., Bopp, L., Arsouze, T., Gehlen, M., & Maury, O. (2015). Spatial and body-size dependent response of marine pelagic communities to projected global climate change. *Global Change Biology*, *21*(1), 154–164. doi: 10.1111/gcb.12679

Lotze, H. K., Tittensor, D. P., Bryndum-Buchholz, A., Eddy, T. D., Cheung, W. W. L., Galbraith, E. D., ... Worm, B. (2019, June). Global ensemble projections reveal trophic amplification of ocean biomass declines with climate change. *Proceedings of the National Academy of Sciences*, *116*(26), 12907–12912. doi: 10.1073/pnas.1900194116

Maury, O. (2010, January). An overview of APECOSM, a spatialized mass balanced

"Apex Predators ECOSystem Model" to study physiologically structured tuna population dynamics in their ecosystem. *Progress in Oceanography*, *84*(1), 113–117. doi: 10.1016/j.pocean.2009.09.013

Maury, O. (2017, August). Can schooling regulate marine populations and ecosystems? *Progress in Oceanography*, *156*(Supplement C), 91–103. doi: 10.1016/j.pocean.2017.06.003

Maury, O., & Poggiale, J.-C. (2013, May). From individuals to populations to communities: A dynamic energy budget model of marine ecosystem size-spectrum including life history diversity. *Journal of Theoretical Biology*, *324*, 52–71. doi: 10.1016/j.jtbi.2013.01.018

Maury, O., Shin, Y.-J., Faugeras, B., Ben Ari, T., & Marsac, F. (2007, September). Modeling environmental effects on the size-structured energy flow through marine ecosystems. Part 2: Simulations. *Progress in Oceanography*, *74*(4), 500–514. doi: 10.1016/j.pocean.2007.05.001

Maury, O., Tittensor, D. P., Eddy, T. D., & Allison, E. H. (2024). The Ocean System Pathways (OSPs): A new scenario framework to investigate the future of oceans. *this issue*.

O'Neill, B. C., Tebaldi, C., van Vuuren, D. P., Eyring, V., Friedlingstein, P., Hurtt, G., ... Sanderson, B. M. (2016, September). The Scenario Model Intercomparison Project (ScenarioMIP) for CMIP6. *Geoscientific Model Development*, *9*(9), 3461–3482. doi: 10.5194/gmd-9-3461-2016

Pörtner, H.-O., & Peck, M. A. (2011). Effects of Climate Change. In *ENCYCLOPEDIA OF FISH PHYSIOLOGY: FROM GENOME TO ENVIRONMENT, VOLS 1-3* (pp. 1738–1745). ELSEVIER ACADEMIC PRESS INC.

Pörtner, H.-O., Roberts, D. C., Tignor, M., Poloczanska, E. S., Mintenbeck, K., Alegría, A., ... Rama, B. (2022). *Climate Change 2022: Impacts, Adaptation, and Vulnerability. Contribution of Working Group II to the Sixth Assessment Report of the Intergovernmental Panel on Climate Change* (Tech. Rep.). IPCC (2022).

Rodgers, K. B., Lin, J., & Frölicher, T. L. (2015, June). Emergence of multiple ocean ecosystem drivers in a large ensemble suite with an Earth system model. *Biogeosciences*, *12*(11), 3301–3320. doi: 10.5194/bg-12-3301-2015

Santana-Falcón, Y., & Séférian, R. (2022, October). Climate change impacts the

vertical structure of marine ecosystem thermal ranges. *Nature Climate Change*, *12*(10), 935–942. doi: 10.1038/s41558-022-01476-5

Schlunegger, S., Rodgers, K. B., Sarmiento, J. L., Ilyina, T., Dunne, J. P., Takano, Y., ... Lehner, F. (2020). Time of Emergence and Large Ensemble Intercomparison for Ocean Biogeochemical Trends. *Global Biogeochemical Cycles*, *34*(8), e2019GB006453. doi: 10.1029/2019GB006453

Sibert, J., Hampton, J., Kleiber, P., & Maunder, M. (2006, December). Biomass, Size, and Trophic Status of Top Predators in the Pacific Ocean. *Science*, *314*(5806), 1773–1776. doi: 10.1126/science.1135347

Tittensor, D. P., Eddy, T. D., Lotze, H. K., Galbraith, E. D., Cheung, W., Barange, M., ... Walker, N. D. (2018, April). A protocol for the intercomparison of marine fishery and ecosystem models: Fish-MIP v1.0. *Geoscientific Model Development*, *11*(4), 1421–1442. doi: 10.5194/gmd-11-1421-2018

Tittensor, D. P., Novaglio, C., Harrison, C. S., Heneghan, R. F., Barrier, N., Bianchi, D., ... Blanchard, J. L. (2021, November). Next-generation ensemble projections reveal higher climate risks for marine ecosystems. *Nature Climate Change*, *11*(11), 973–981. doi: 10.1038/s41558-021-01173-9

Ying, J., Collins, M., Cai, W., Timmermann, A., Huang, P., Chen, D., & Stein, K. (2022, April). Emergence of climate change in the tropical Pacific. *Nature Climate Change*, *12*(4), 356–364. doi: 10.1038/s41558-022-01301-z

Figure 9.

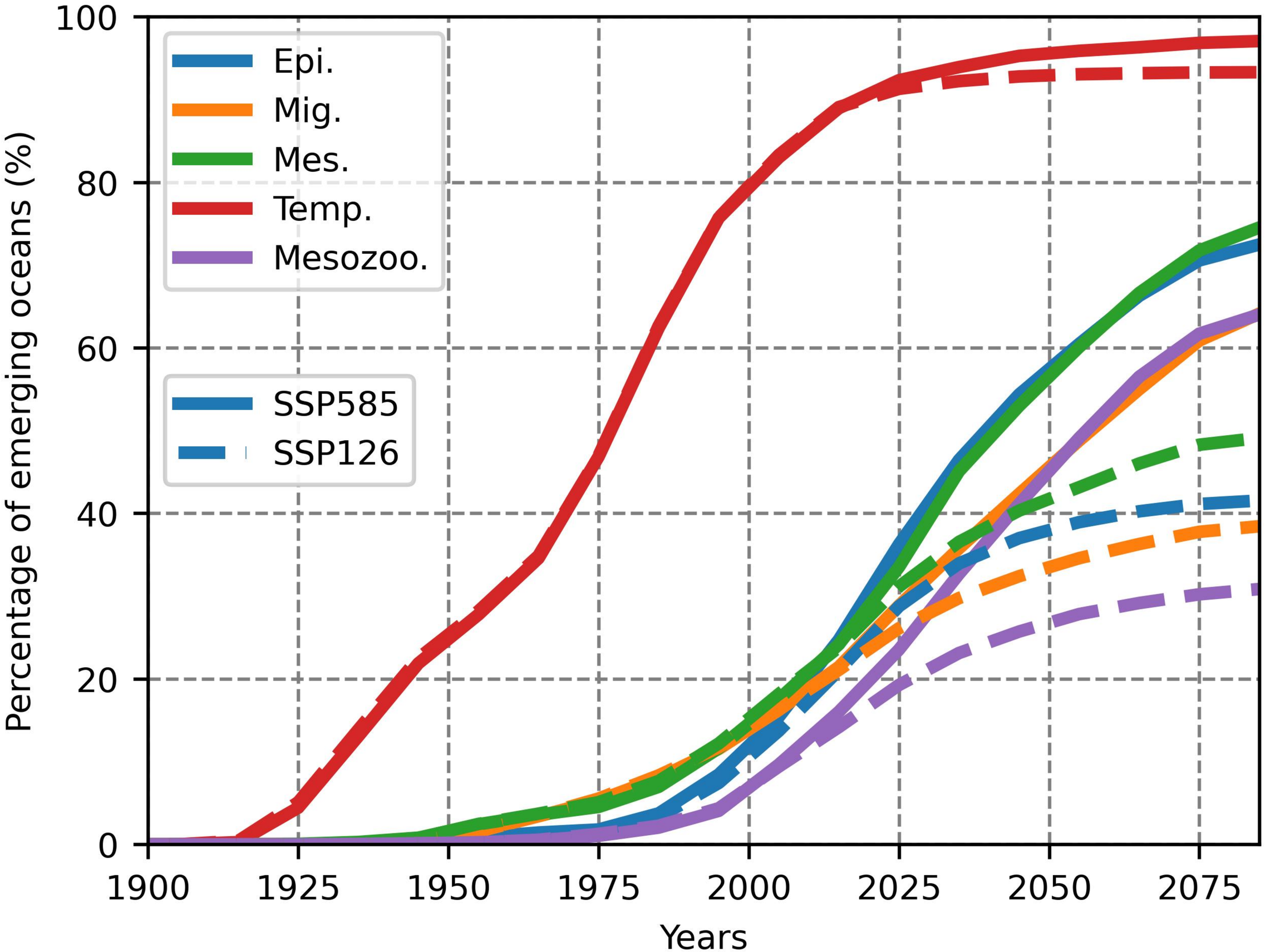
Epi.
Mig.
Mes.
Temp.
Mesozoo.
SSP585
SSP126
Percentage of emerging oceans (%)
0
20
40
60
80
100
1900
1925
1950
1975
2000
2025
2050
2075
Years

Figure 1.

Raw time-series

a)

%

Members 1
Members 2
Members 3
Members 4
Members 5
Members 6
Member mean
C.C signal

Gaussian kernel

b)

Y_0

Weight

Years

Anomaly time-series

c)

%

TOE

d)

%

Figure 4.

Temp.
Mesozoo.
Percentage of emerging cells (%)
Integrated percentage of emerging cells (%)
0
5
10
15
0
20
40
60
80
100

Epi.
Mig.
Mes.
Percentage of emerging cells (%)
Integrated percentage of emerging cells (%)
0
5
10
15
0
20
40
60
80
100
[1900, 1910[
[1910, 1920[
[1920, 1930[
[1930, 1940[
[1940, 1950[
[1950, 1960[
[1960, 1970[
[1970, 1980[
[1980, 1990[
[1990, 2000[
[2000, 2010[
[2010, 2020[
[2020, 2030[
[2030, 2040[
[2040, 2050[
[2050, 2060[
[2060, 2070[
[2070, 2080[
[2080, 2090[

Figure 3.

TOE, Epi.
TOE, Mig.
TOE, Mes.
Years
2000
1950
2050
a)
b)
c)
Late emergence
Early emergence
SNR, Epi.
SNR, Mig.
SNR, Mes.
10
15
0
2
4
5
d)
e)
f)
Increase
Decrease
SNR decrease
SNR increase
S, Epi.
S, Mig.
S, Mes.
%
30
40
50
20
g)
h)
i)
S increase
S decrease
N, Epi.
N, Mig.
N, Mes.
3.5
3.0
2.5
2.0
1.5
1.0
j)
k)
l)
N increase
N decrease
10^0
10^1
Length (cm)

Figure 2.

SST

Temp (500-1000m)

Mesozoo

a

b

c

SSP5.85

SSP1.26

Celcius

Celcius

%

Epi.

Mig.

Mes.

d

e

f

%

%

%

1850 1900 1950 2000 2050

1850 1900 1950 2000 2050

1850 1900 1950 2000 2050

Figure 8.

Epipelagic

b)

Epipelagic

e)

Migrants

c)

Migrants

f)

Mesopelagic

d)

Mesopelagic

g)

1950 1970 1990 2010 2030 2050 2070 2090

TOE

−90 −60 −30 0 30 60 90

Relative signal (%)

Figure 6.

Time of emergence

a)

1930 1970 2010 2050 2090

|Signal| to Noise ratio

b)

0 4 8 12 16 20

Noise

c)

0.0 0.2 0.4 0.6 0.8 1.0

C

Signal

d)

−6 −4 −2 0 2 4 6

C

Figure 7.

Time of emergence

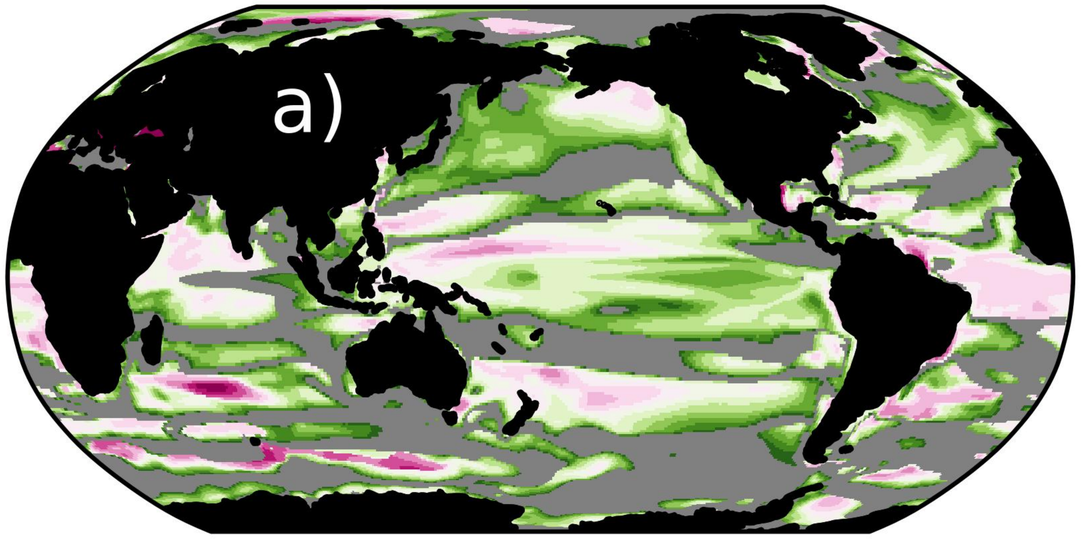

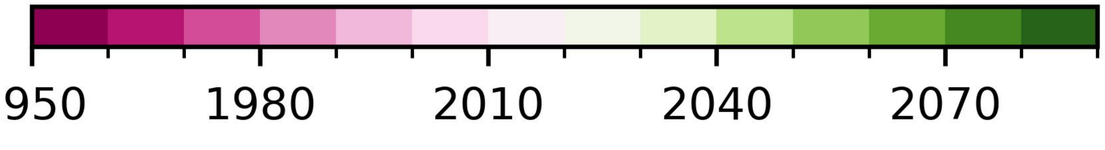

|Signal| to Noise ratio

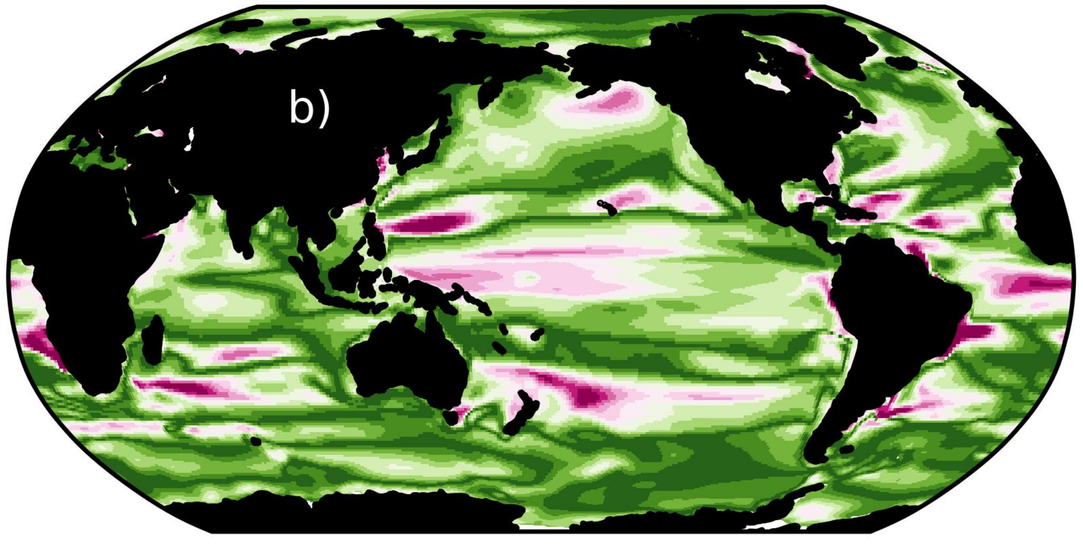

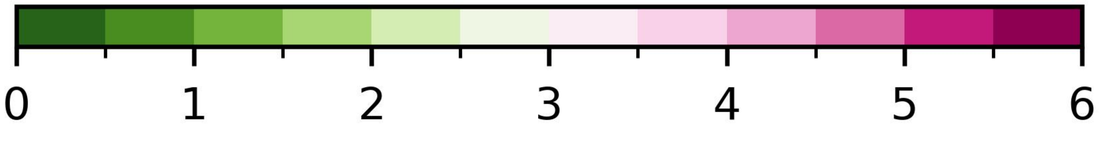

Relative Noise

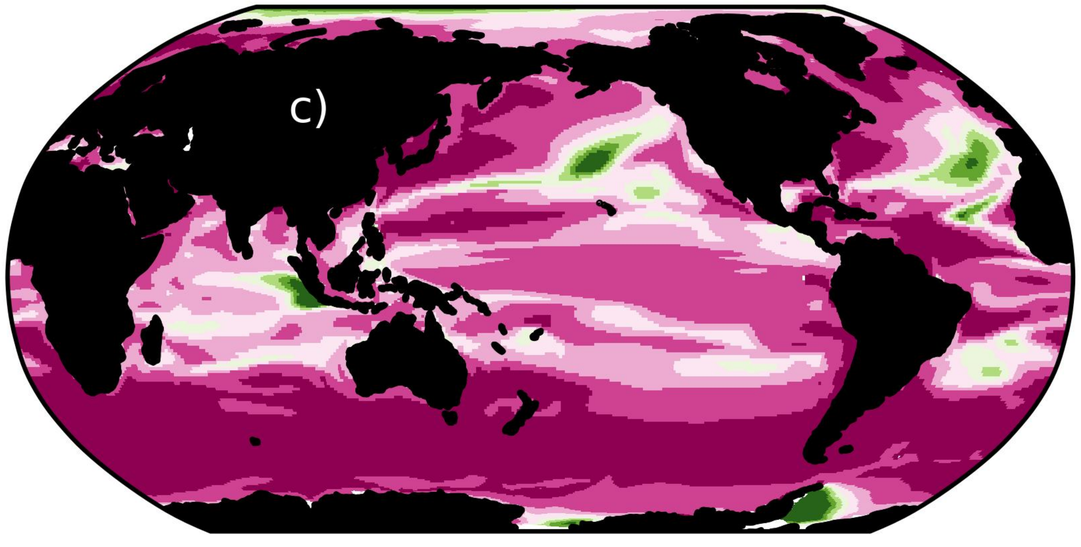

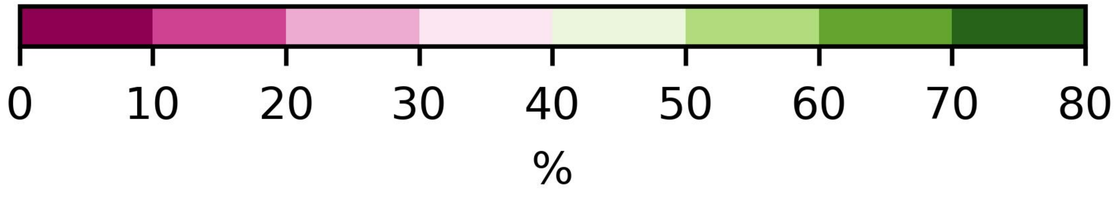

Relative Signal

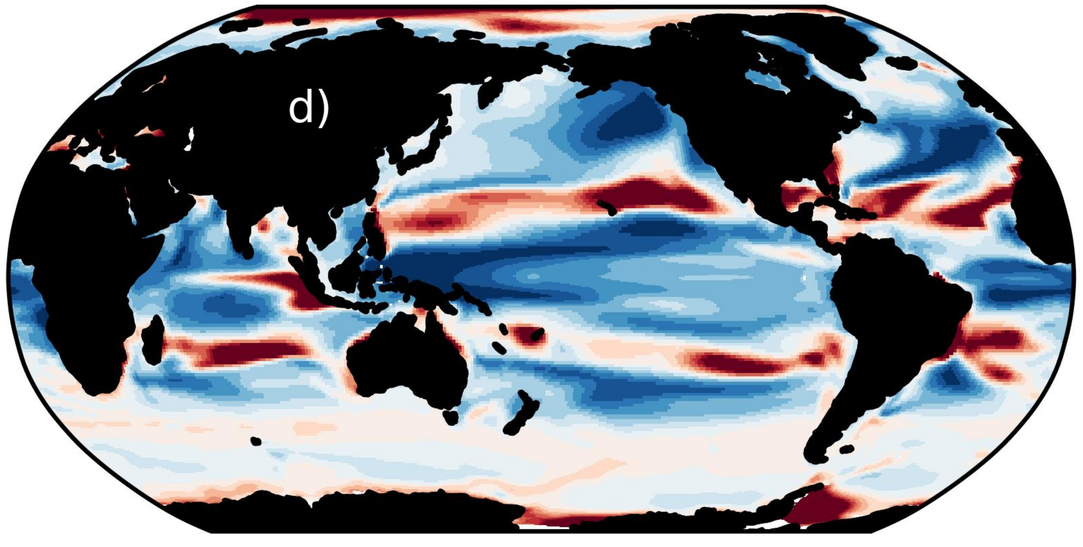

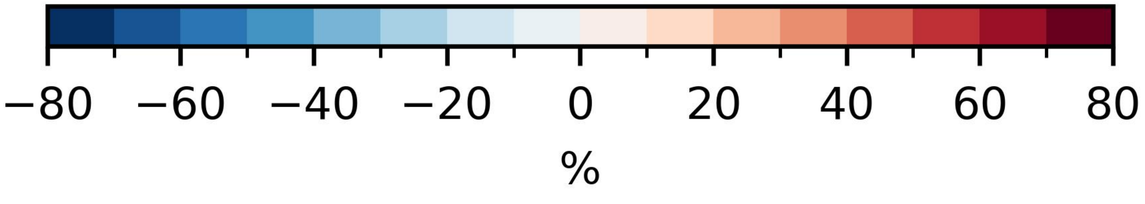

Figure 5.

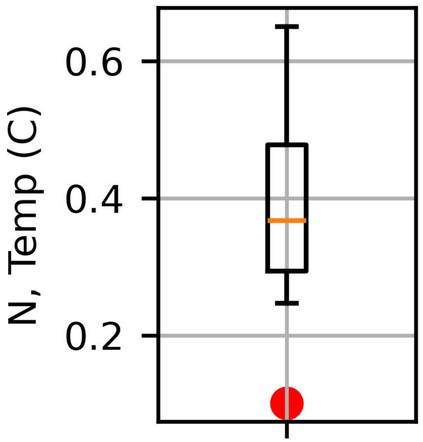
N, Temp (C)
0.6
0.4
0.2

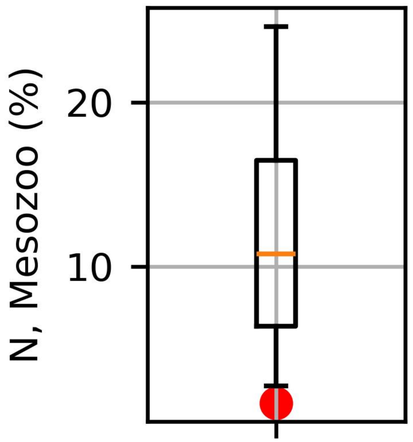
N, Mesozoo (%)
20
10

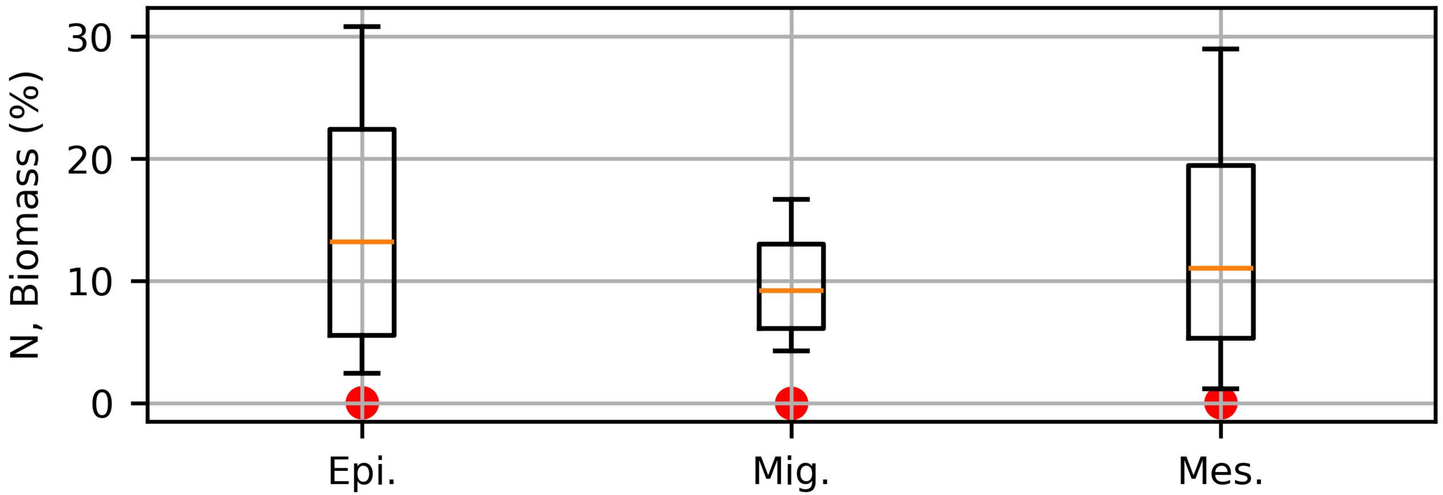
N, Biomass (%)
30
20
10
0
Epi.
Mig.
Mes.

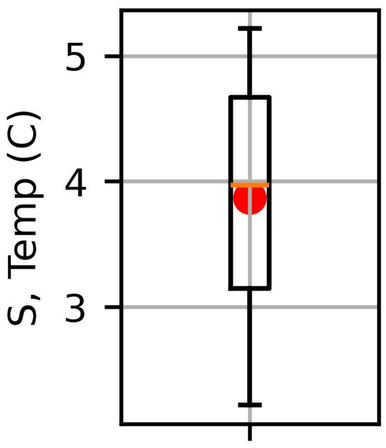
S, Temp (C)
5
4
3

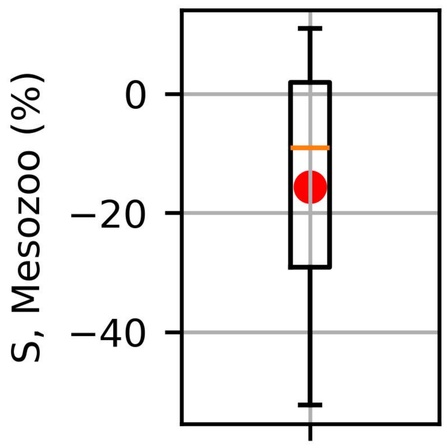
S, Mesozoo (%)
0
−20
−40

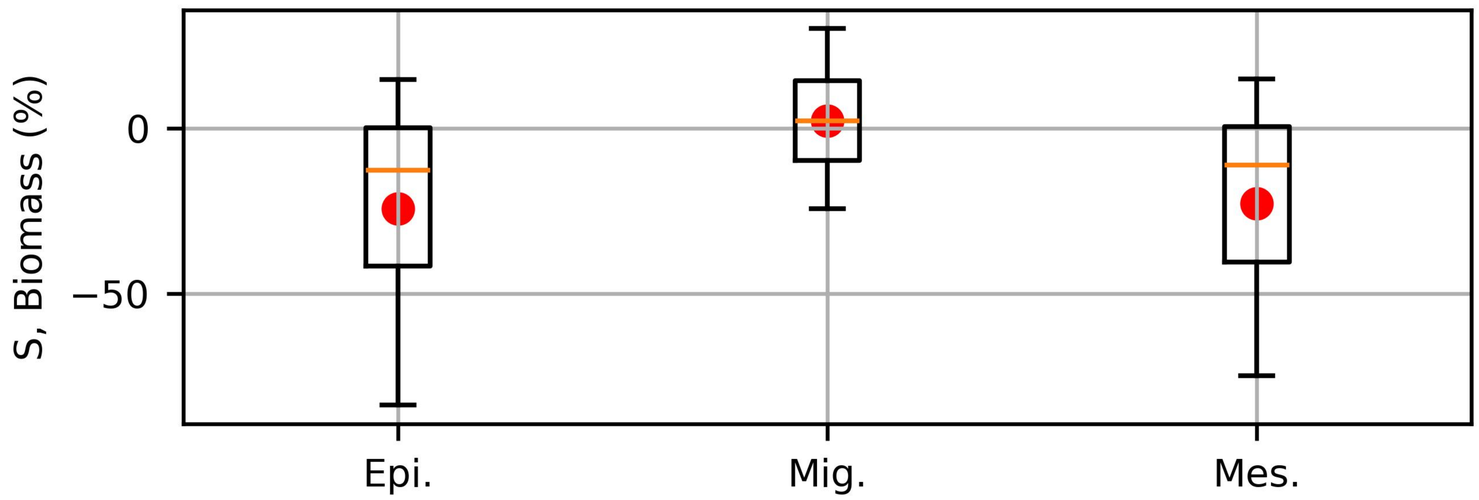
S, Biomass (%)
0
−50
Epi.
Mig.
Mes.

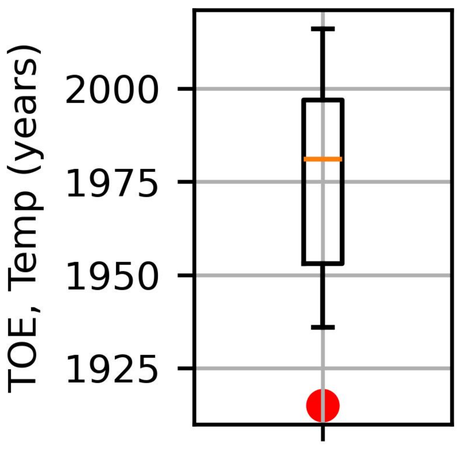
TOE, Temp (years)
2000
1975
1950
1925

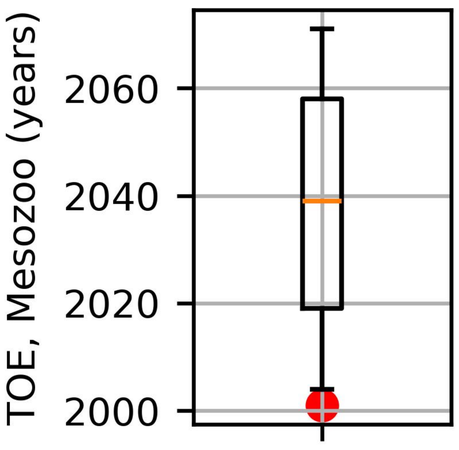
TOE, Mesozoo (years)
2060
2040
2020
2000

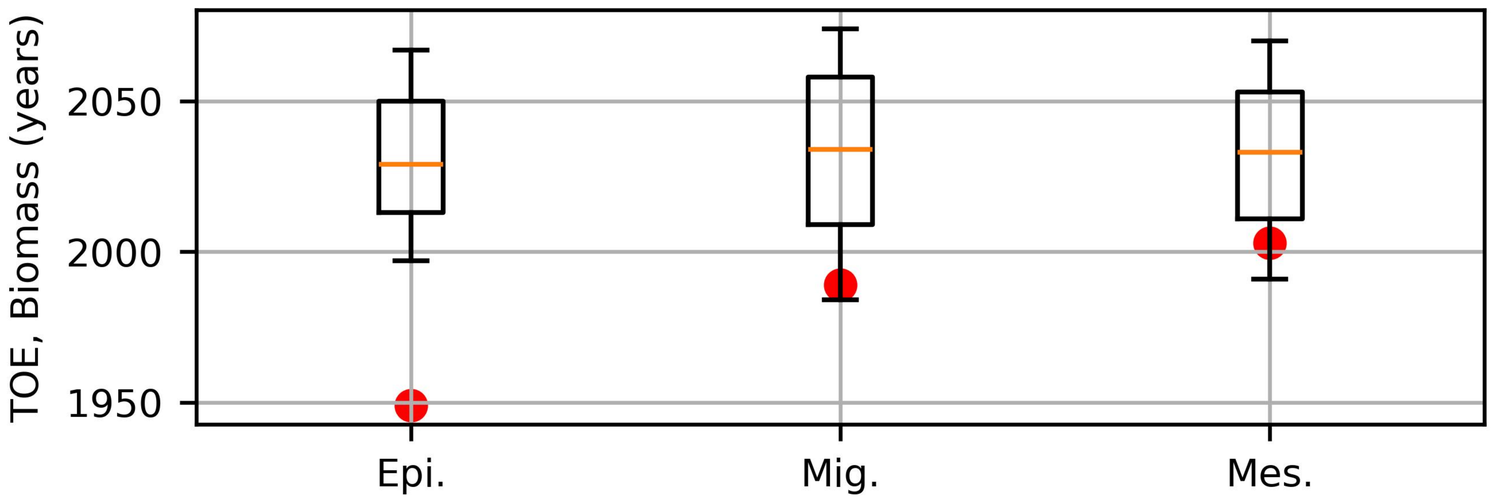
TOE, Biomass (years)
2050
2000
1950
Epi.
Mig.
Mes.